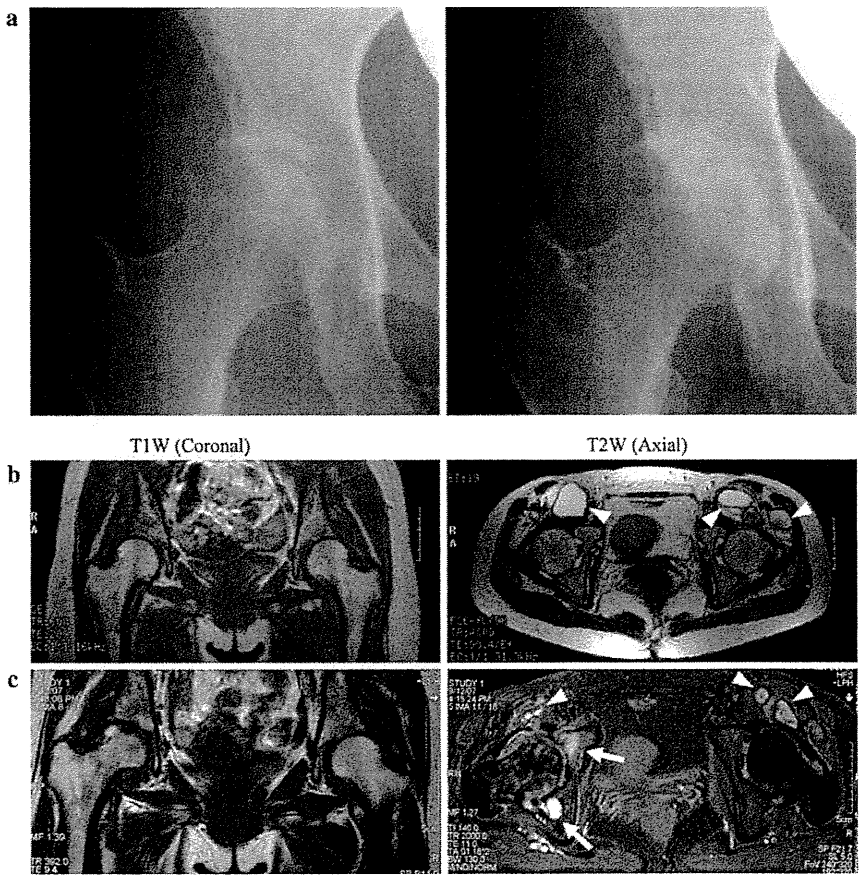

Fig. 4 X-ray and coronal T1-weighted (*left*) and axial T2-weighted (*right*) MR images of the hip joints. **a** X-ray in December 2005 (*right*) and September 2007 (*left*). **b** MRI in January 2005 only showed extracapsular cyst (*arrowheads*). **c** MRI in September 2007 showed not only extracapsular cysts (*arrowheads*) but also joint destruction accompanied with cyst-like formation (*arrows*)

Discussion

Joint involvement often occurs in SLE, ranging from minor arthralgia to severe deforming arthritis, or so-called Jaccoud's arthropathy [8]. An important difference between the joint involvements in SLE and RA is that arthropathy in SLE is nonerosive. However, some groups have recently described erosive arthritis manifested in finger joints of SLE patients, which they call "Rhupus hand." van Vugt et al. [6] also reported joint erosion detected in SLE patients by X-ray. Moreover, MRI and ultrasound imaging were reported as being helpful to distinguish joint involvement in SLE patients that could not be detected by X-ray [9, 10]. However, it is still controversial whether such patients represent an erosive subtype of SLE arthritis, an overlap of SLE and RA, or a true coexistence of SLE and RA. In this case, the patient did not reach the criteria of RA during the whole course of the disease. We could not deny the possibility that the symptoms of RA might have been masked because the patient was treated with 10–20 mg/day prednisone, but laboratory examinations such as the negatives of RF and anti-CCP antibodies indicated that she was not RA.

This patient was diagnosed with dermatomyositis (DM) by clinical findings, increased muscular enzymes, electromyography, and histopathology, although the anti-Jo-1 antibodies were negative. Anti-aminoacyl-tRNA synthetase antibodies were not examined. Bradley et al. [11] has reported the association of Jaccoud arthropathy with DM. However, erosive arthritis was rarely manifested in DM. Shultz et al. [12] reported that distal joints such as the wrist and finger joints were only occasionally affected with an erosive arthritis in dermatomyositis which was associated with periarticular calcification due to apatite deposition. The involvement of proximal joints has rarely been reported [13]. Therefore, our patient was unique even among patients with DM in that she developed severe erosive arthritis which affected both the wrist and the hip joints.

Bursitis is considered as a differential diagnosis for the extracapsular cyst. Because the bursae around the wrist are generally the ones of synovial sheaths of the carpal flexor and extensor tendons, the bursitis of the wrist must manifest inflammatory changes around the affected tendons [14]. However, the MRI (Fig. 2a) revealed no remarkable

involvement of tendon sheaths, which led us to diagnose the tumorous formation as an extracapsular cyst.

Concerning the involvement of the hip joint in SLE, aseptic necrosis of femoral head (AVN) is a common and severe complication of steroid use [15]. The prevalence of AVN in SLE is 15–20% and treatment with high-dose corticosteroids has been reported as one of the most dominant risk factors. In contrast, in this case, no findings of AVN were detected by X-ray, by MRI or even by histological examination. Instead, this case showed erosive joint destruction of the hip accompanied by extracapsular cysts that resembled the involvement of the wrist joint. Previously a report described progressive destruction of the knee joint due to SLE which resulted in total knee replacement [16]. However, hip joint involvement due to SLE itself seems extremely rare. Another recent report presented a case of nonrheumatoid erosive arthritis of the hip and the wrist joints associated with type I hereditary angioedema (HAE), with unknown etiology, which resulted in THR [17]. Type I HAE has been described in association with several rheumatic and autoimmune disorders including SLE. In this disease, the serum levels of C1q and C3 are normal while C2 and C4 are usually decreased [18]. In the present case, C1q, C3, and C4 were all decreased, which was incoherent to the entity of type I HAE. Therefore, it was reasonable to consider that destructed hip joint was caused by the same etiology as that of her wrist joint, not by type I HAE. To our knowledge, this is the first report of erosive arthritis in SLE involving the hip joint without AVN.

Unfortunately, the pathophysiology was not determined even by histopathological examinations. A series of examinations in this case showed similar findings of chronic synovial arthritis. These findings were compatible not only with RA but also with osteoarthritis due to the lack of RA-specific findings such as lymph follicle formation or rheumatoid nodule. The evaluation of joint capsules or articular ligaments may have revealed the pathological changes indicating SLE arthropathy if samples were collected, but the lack of such well-known histological features itself may indicate this rare but noteworthy entity.

While several erosive arthropathy cases in SLE were reported with diagnostic imaging, few reports have described the course of surgical treatment for SLE arthritis. In this case three surgical operations were performed on her left wrist joint. The cyst on the wrist reappeared after two surgical operations of cystectomy and partial synovectomy. Finally, complete cure was achieved after the drastic resection of eroding synovium. This means that the extracapsular cyst was caused secondary to the aggressive synovitis of the wrist joint. Moreover, this case presented the similar extracapsular cyst formation and joint destruction in the right hip joint. Taken together, the course of this patient indicates an aggressive synovitis that caused joint destruction in multiple joints in SLE without apparent concomitant RA involvement, shedding light on the understanding of pathogenesis of erosive arthritis in SLE.

In summary, we carried out surgical treatments of erosive non-RA arthritis in SLE. Even extensive histopathological studies did not show RA involvement or osteonecrosis. The synovial arthropathy was clinically aggressive, and a drastic synovectomy and a joint replacement led to complete symptom relief. Rheumatologists should be aware of the possibility of this entity. A careful assessment of joint synovitis is essential to plan the surgical involvement for SLE arthropathy.

Conflict of interest statement None.

References

1. Cohen AS, Reynolds WE, Franklin EC, Kulka JP, Ropes MW, Shulman LE, et al. Preliminary criteria for the classification of systemic lupus erythematosus. Bull Rheum Dis. 1971;21:643–4.
2. Tan EM, Cohen AS, Fries JF, Masi AT, McShane DJ, Rothfield NF, et al. The 1982 revised criteria for the classification of systemic lupus erythematosus. Arthritis Rheum. 1982;25:1271–7.
3. Girgis FL, Ppple AW, Bruckner FE. Jaccoud's arthropathy. A case report and necropsy study. Ann Rheum Dis. 1978;37:561–5.
4. Spronk PE, ter Borg EJ, Kallenberg CG. Patients with systemic lupus erythematosus and Jaccoud's arthropathy: a clinical subset with an increased C reactive protein response? Ann Rheum Dis. 1992;51:358–61.
5. Martini A, Ravelli A, Viola S, Burgio RG. Systemic lupus erythematosus with Jaccoud's arthropathy mimicking juvenile rheumatoid arthritis. Arthritis Rheum. 1987;30:1062–4.
6. van Vugt RM, Derksen RH, Kater L, Bijlsma JW. Deforming arthropathy or lupus and rupus hands in sustemic lupus erythematosus. Ann Rheum Dis. 1998;57:540–4.
7. Fernández A, Quintana G, Rondón F, Restrepo JF, Sánchez Á, Matteson EL. Lupus arthropathy: a case series of patients with rhupus. Clin Rheumatol. 2006;25:164–7.
8. Santiago MB, Galvão V. Jaccoud arthropathy in systemic lupus erythematosus: analysis of clinical characteristics and review of the literature. Medicine. 2008;87:37–44.
9. Ostendorf B, Schener A, Specker C, Mödder U, Schneider M. Jaccoud's arthropathy in systemic lupus erythematosus: differentiation of deforming and erosive patterns by magnetic resonance imaging. Arthritis Rheum. 2003;48:157–65.
10. Saketkoo LA, Quinet R. Revising Jaccoud arthropathy as an ultrasound diagnosed erosive arthropathy in systemic lupus erythematosus. J Clin Rheumatol. 2007;13:322–7.
11. Bradley JD. Jaccoud's arthropathy in adult dermatomyositis. Clin Exp Rheumatol. 1986;4:273–6.
12. Shultz E, Barland P. Erosive arthritis with dermatomyositis without elevated anti-Jo-antibodies and not associated with pain. J Rheumatol. 1993;20:597–9.
13. Mok CC, Tsui EY, Chau SY. Erosive arthropathy in amyopathic dermatomyositis. Clin Exp Rheumatol. 2003;21:409–10.
14. Gray's anatomy. The anatomical basis of medicine and surgery. 38th ed.,1995. p. 852–4.
15. Orban H, Cirstoiu C, Adam R. Total hip arthroplasty in secondary systemic lupus erythematosus femoral head avascular necrosis. Rom J Intern Med. 2007;45:123–9.

16. Yanase M, Koshino T, Mitsuhashi S, Takeuchi R, Yamamoto K, Saitoh T. Destructed knee in patient with systemic lupus erythematosus treated with total knee arthroplasty: a case report (in Japanese). Ryumachi. 2001;41:751–5.
17. Palazzi C, D'amico E, Cacciatore P, Pennese E, Olivieri I. Non-rheumatoid erosive arthritis associated with type I hereditary angioedema. Clin Rheumatol. 2005;24:632–3.
18. Nzeako UC, Frigas E, Tremaine WJ, et al. Hereditary angioedema: a broad review for clinicians. Arch Intern Med. 2002;161(20):2417–29.

Leukemia Research 33 (2009) 649–654

Contents lists available at ScienceDirect

Leukemia Research

journal homepage: www.elsevier.com/locate/leukres

Aberrant somatic hypermutations in thyroid lymphomas

Tetsuya Takakuwa[a,*], Akira Miyauchi[c], Katsuyuki Aozasa[b]

[a] Human Health Science, Kyoto University Graduate School of Medicine, 606-8507 Sakyo-ku, Shogoin Kawahara-cyo 53, Kyoto, Japan
[b] Department of Pathology, Osaka University Graduate School of Medicine, Osaka, Japan
[c] Department of Surgery, Kuma Hospital, Kobe, Japan

ARTICLE INFO

Article history:
Received 8 May 2008
Received in revised form 6 October 2008
Accepted 7 October 2008
Available online 18 November 2008

Keywords:
Thyroid lymphoma
Follicular lymphoma
Aberrant somatic hypermutation

ABSTRACT

To determine a possible role of aberrant somatic hypermutation (ASHM) in the pathogenesis of thyroid lymphoma (TL), mutational status of genes affected by ASHM, including *c-MYC*, *PIM-1*, *PAX-5* and *RhoH/TTF*, was analyzed. Tumor specimens from 33 patients with thyroid B-cell lymphoma and 14 with chronic lymphocytic thyroiditis (CLTH), an autoimmune thyroiditis known to provide a basis for TL development, was examined. Mutations of at least one of these genes was detected in 16 of 33 (48.5%) patients with TL and in 2 of 14 (14.3%) CLTH. Occurrence of ASHM in *PIM-1*, *RhoH/TTF*, and c-*MYC* was a constant finding in follicular lymphoma (FL) (all of 11 cases) but not so frequent in diffuse large B-cell lymphoma (DLBCL) (4 (33.3%) of 12 cases) and Marginal zone B-cell lymphoma (MZBCL) (1 (10.0%) of 10 cases). ASHM activity is ongoing in most of FL and DLBCL because intraclonal variants were found. FL was also unique in its lower expression level of activation-induced cytidine deaminase, a main player in DNA-modifying processes during SHM, compare to DLBCL and MZBCL.

1. Introduction

Somatic hypermutation (SHM) in the germinal center (GC) B-cells is a process that enhances affinity of antibody for a particular antigen by introducing nucleotide substitutions within the immunoglobulin variable region (IgHV) genes [1]. SHM is characterized by the predominance of single base substitutions, preference for transitions over transversions, and specific targeting of AG/G/CT/AT (RGYW) motifs. *BCL-6* proto-oncogene, a transcriptional repressor that regulates B-cell maturation [2], is another target of SHM in GC B-cells. BCL-6 is a proto-oncogene initially cloned from 3q27 breakpoints in diffuse large B-cell lymphoma (DLBCL) of the immunocompetent host, and found to encode a zinc-finger transcriptional repressor.

An aberrant activity of SHM, called aberrant SHM (ASHM), has been suggested to contribute to the development of DLBCLs [3]. Majority of DLBCLs exhibit ASHM in the coding sequence or 5′ untranslated region (UTR) of proto-oncogenes, including *PIM-1*, *PAX-5*, *RhoH/TTF*, and c-*MYC* [3], which is implicated in the pathogenesis of lymphoid malignancies. The ASHM of these genes was reported to be commonly found in DLBCL but uncommon in other kinds of GC-derived lymphomas such as follicular lymphoma (FL) and Burkitt lymphoma. This observation might lead to the concept that ASHM plays a role for lymphomagenesis of aggressive B-cell lymphomas through mutation of multiple proto-oncogenes. Recent study, however, demonstrated that ASHM was also observed in various kinds of lymphomas, i.e., lymphoma associated with AIDS [4], primary central nervous system lymphomas [5], mediastinal DLBCL [6,7], and hepatitis C virus positive non-Hodgkin's B-cell lymphoma (B-NHL) [8], cutaneous B-cell lymphoma [9], lymphoma of marginal zone B-cell type (MZBCL) and extranodal DLBCL [10], and FL [11], suggesting that ASHM may contribute to oncogenesis in a wide spectrum of B-cell lymphomas.

Thyroid lymphoma (TL) is a minor constituent of B-NHL, accounting for 2.2–2.5% of all cases of extranodal lymphomas [12,13]. TL had attracted the attention of investigators because of its putative origin from active lymphoid cells in an organ-specific autoimmune thyroiditis, i.e., Hashimoto's thyroiditis or chronic lymphocytic thyroiditis (CLTH) [14,15]. TL exclusively comprise B-NHL with DLBCL, MZBCL and FL being frequent in the order [16]. Previous study revealed the relatively high level of SHM (1–21%, average 12%) in IgHV genes [17], and deviated VH4 Ig gene usage among MZBCL in TL [18]. In this study, biopsy specimens from 33 patients with B-NHL of thyroid and 14 CLTH patients were analyzed to evaluate occurrence of ASHM. Activation-induced cytidine deaminase (*AID*) and *POL-eta* gene, known to play central roles in the DNA-modifying processes during SHM, contribute differently and complementarily to this process [19–22] Then, expression levels of *AID* and *POL-eta* gene and their relation with the ASHM were also analyzed.

* Corresponding author. Tel.: +81 75 751 3956; fax: +81 75 751 3956.
E-mail address: tez@hs.med.kyoto-u.ac.jp (T. Takakuwa).

0145-2126/$ – see front matter © 2008 Elsevier Ltd. All rights reserved.
doi:10.1016/j.leukres.2008.10.007

2. Patients and methods

2.1. Patients

Thirty-three patients with TL and 14 with CLTH, who underwent surgical resection including total, partial thyroidectomy, or open biopsy of thyroid lesions in the Kuma Hospital, Kobe, Japan, during the period 1995–1999, were enrolled in this study with informed consent. TL patients consisted of 7 males and 26 females while CLTH patients consisted of 1 male and 13 females. Age of patients on admission ranged from 27 to 84 (median 65) years in TL and 45 to 75 (median 62.5) years in CLTH. All 33 tissue specimens were subdivided into two: one for snap-frozen at −150 °C and another for formalin fixed paraffin embedded for further analysis. Criteria for the diagnosis of CLTH included increased consistency of the thyroid-gland, occasional hypothyroidism, high level of thyroid-stimulating hormone, low ^{123}I-uptake, and the presence of antimicrosomal and/or anti-thyroglobulin antibodies in the serum. Histologic findings of CLTH included lymphocytic infiltration, usually forming lymphoid follicles with GCs, varying degrees of fibrosis and oxyphilic change or squamous metaplasia in epithelial cells of the thyroid follicles. All of the histologic sections from TL cases were reviewed by one of the authors (KA) and were classified according to the 2001 World Health Organization (WHO) Classification of Tumours of Haematopoietic and Lymphoid Tissues [16]. They included 12 DLBCLs, 10 MZBCLs, and 11 FLs. Immunohistochemical study on the paraffin sections from TL was carried out using the avidin–biotin–peroxidase complex (ABC) method. Monoclonal antibodies used for immunophenotyping were CD20, CD3, BCL-6, MUM1 (Dakocytomation, Glostrup, Denmark, dilution at 1:400, 1:50, 1:50, 1:50, respectively), and CD10 (NICHIREI BIOSCIENCES, Tokyo, Japan, used as a prediluted antibody). All TL were of B-cell lineage. Morphological and immunophenotypic analyses revealed that the fraction of malignant cells in the pathological specimen was 90% or more in all cases. DLBCL was stratified into 3 germinal center B-cell-like (GCB) and 9 non-GCB phenotypes according to the immunophenotype of CD10, BCL-6 and MUM-1 [23]. t(14;18) with BCL-2-IgH rearrangement was detected in 4 (36.4%) of 11 FL cases using the method described elsewhere [24]. Translocation t(14;18) as a hallmark of FL was reported to occur at a lower frequency, 48–55%, in Asian patients, than in the European and Northern American patients (70–95%) [16,19–25]. The reactive and non-neoplastic nature of CLTH lesions was confirmed by clonality assays [24,26].

2.2. Detection of ASHM

DNA was extracted from fresh frozen thyroid tissues, using the phenol-chloroform extraction method. Sequences of the oligonucleotide primers used for amplification of *PIM-1*, *PAX-5*, *RhoH/TTF*, exons 1 and 2 of *c-MYC*, and *BCL-6* by the polymerase chain reaction (PCR) were described elsewhere [5,8].

2.3. Analysis of PIM-1, PAX-5, RhoH/TTF, c-MYC, and BCL-6 mutations

Mutational analysis of *PIM-1*, *PAX-5*, *RhoH/TTF*, *c-MYC*, and *BCL-6* was confined to the regions where more than 90% of mutations introduced by ASHM were reported to be found in B-cell lymphomas [3,4,11]. Purified PCR products were sequenced using an ABI 3100 Genetic Analyser (Applied Biosystems, Foster City, CA, USA) with the dye-terminator protocol. Both strands of each PCR product were sequenced. The sizes of PCR products for the *PIM-1*, *PAX-5*, *RhoH/TTF*, *c-MYC* exon 1, *c-MYC* exon 2, and *BCL-6* were 1025, 932, 875, 1302, 1167, and 739 bp, respectively. The sequences of each PCR product were compared with the corresponding wild-type sequence. GenBank accession numbers of wild-type *PIM-1*, *PAX-5*, *RhoH/TTF*, *c-MYC*, and *BCL-6* sequences are AF386792, AF386791, AF386789, X00364, and AF191831, respectively.

To analyze the presence of intraclonal heterogeneity, sequencing of cloned PCR products of *PIM-1*, *PAX-5*, *RhoH/TTF* and *BCL-6* was performed using the proof-reading Pfu polymerase (Invitrogen, Rockville, MD). From each patient, 20 clones were sequenced from both sides. The mutations detected at least in two individual sequencing of each patient were considered to be ongoing mutation.

2.4. Real-time PCR for assessment of expression levels of AID and POL-eta genes

Tissue samples from TL and CLTH were homogenized, and total RNA was extracted in the presence of TRIzol reagent (Invitrogen, Rockville, MD). Five microgram of total RNA were reverse-transcribed by random hexamer priming. Expression levels of *AID* and *POL-eta* were analyzed using the TaqMan Gene Expression Assays TM according to the protocol of the manufacturer (Applied Biosystems). The primers used were: *AID*, ID Hs00221068_m1, POL-eta; Hs00197814_m1, human GAPD; 4352934E (Applied Biosystems). Standard curves for quantification of the molecules were constructed from the results of simultaneous amplifications of serial dilutions of cDNA from tonsilar tissues of healthy volunteer. Real-time PCR and subsequent calculations were carried out with an ABI Prism 7700 Sequence Detector System (Applied Biosystems). To normalize the differences in RNA degradation and RNA loading for reverse transcription-PCR in individual samples, the expression levels of each molecule were divided by that of human GAPD in the same samples. All experiments were performed at least in duplicate. The expression level of each gene in tonsil was defined as 100, and the relative gene expression levels in each case was compared.

2.5. Statistical analysis

Differences in the frequency of mutations were defined as statistically significant when the p values were less than 0.05. Mutation frequency was normalized based on the base composition of the sequences of each gene analyzed. The normalized mutation frequencies of each individual nucleotide were compared with the expected mutation frequency by Chi-square test [4]. The mutation frequency for nucleotides occurring in the context of an RGYW/WRCY motif was compared with the expected mutation frequency by the Chi-square test [4]. AID expression among histological subtypes of TL were compared by Kruskal–Wallis test then by Sheffe's F-test. Levels of AID expressions between ASHM positive and negative cases were compared by t-test.

3. Results

3.1. Frequency of ASHM in TL and CLTH

DNA extracted from the biopsy specimens from 33 TL patients and 14 CLTH patients were analyzed for mutations of *PIM-1*, *PAX-5*, *RhoH/TTF*, and *c-MYC* (Table 1). Mutations of *PIM-1*, *PAX-5*, *RhoH/TTF*, and *c-MYC* were detected in 7 (21.2%), 2 (6.1%), 7 (21.2%), and 11 (33.3%) of 33 TL patients, respectively. Mutations of at least one of these genes was detected in 16 of 33 (48.5%) TL patients and in 2 of 14 (14.3%) CLTH.

Frequency of mutations in more than one of these genes in FL (11 of 11 (100%)) was significantly higher than that in MZBCL (1 of 10 (10.0%)), DLBCL (4 of 12 (33.3%)), and CLTH (2 of 14 (14.3%)). Frequency of mutations was not different between GC (1 of 3 (33.3%)) and non-GC (3 of 9 (33.3%)) subtypes in DLBCL. Frequency of mutations in *c-MYC* and *PIM-1* was significantly higher in FL (*c-MYC*, 63.6%; *PIM-1*, 45.5%) than in MZBCL (*c-MYC*, 10.0%; *PIM-1*, 0%) and CLTH (*c-MYC*, 7.1%; *PIM-1*, 0%). Mutations of *RhoH/TTF* were significantly higher in FL (63.6%) than in MZBCL (0%), CLTH (7.1%) as well as DLBCL (0%).

3.2. Distribution of mutations in PIM-1, PAX-5, RhoH/TTF, and c-MYC in TL tissue

Characteristics of *PIM-1*, *PAX-5*, *RhoH/TTF*, and *c-MYC* mutations in each case of TL and CLTH were shown in Table 2, and their general features are summarized in Table 3. Average frequency of mutations per 1000 bp in cases with mutations ranged from 0.86 (c-MYC exon 2) to 4.35 (c-MYC exon 1). Majority of the mutations were single base-pair substitutions ($n = 58$). Deletions/insertions of a short DNA stretch were observed in three cases (Tables 2 and 3). Of the 58 single base-pair substitutions, 30 were transitions and 28 were transversions, with a transition-to-transversion ratio of 2.18 (expected 1.07, $p < 0.05$, Chi-square test; Table 3). Analysis of the nucleotide mutational pattern in *PIM-1*, *PAX-5*, *RhoH/TTF*, and *c-MYC* revealed that G+C and A+T base-pairs were equally targeted. Mutations within RGYW/WRCY motifs were more frequent than mutations without these motifs in c-MYC exon 1 ($p = 0.023$) (Table 3).

Three c-MYC mutations found in TL and one in CLTH involved the coding region. Two of these mutations would cause amino acid changes (Val → Ala in F6, Ile → Thr in H7), which result in alteration of the biochemical and structural properties of the proteins. Whereas the remaining two mutations were silent, one PIM-1 mutation in FL was located within the coding region, which would cause an amino acid change (Ala → Thr in F6), probably altering the biochemical and structural properties of the protein.

3.3. BCL-6 mutations in TL

The mutational analysis of the BCL-6 gene was also performed in all 33 TL patients. SHM of BCL-6 were detected in 22 of 33 (66.6%) cases: including 8 of 11 (72.7%) in FL, 9 of 12 in DLBCL (75.0%), 5

Table 1
Distribution of PIM-1, PAX-5, RhoH/TTF, c-MYC and BCL-6 mutations in thyroid lymphomas and chronic lymphocytic thyroiditis.

Histology	Mutated/tested (%)					
	c-MYC exon 1 and 2	RohH/TTF	PIM-1	PAX-5	Any	BCL-6
CLTH	1/14 (7.1%)	1/14 (7.1%)	0/14	0/14	2/14 (14.3%)	2/14 (14.3%)
Lymphoma (all)	11/33 (33.3%)	7/33 (21.2%)	7/33 (21.2%)	2/33 (6.1%)	16/33 (48.5%)a	22/33 (66.7%)a
FL	7/11 (63.6%)a,b	7/11 (63.6%)a,b,c	5/11 (45.5%)a,b	1/11 (9.1%)	11/11 (100%)a,b,c	8/11 (72.7%)a
MZBCL	1/10 (10.0%)	0/10	0/10	0/10	1/10 (10.0%)	5/10 (50.0%)
DLBCL	3/12 (25.0%)	0/12	2/12 (16.7%)	1/12 (8.3%)	4/12 (33.3%)	9/12 (75.0%)a

CLTH, chronic lymphocytic thyroiditis; FL, follicular lymphoma; DLBCL, diffuse large B-cell lymphoma; MZBCL, merginal zone B-cell lymphoma.
a, vs chronic lymphocytic thyroiditis; b, vs MZBCL; c, vs DLBCL: statistically significant by Chi-square test.

Table 2
Mutational analysis of c-MYC, RhoH/TTF, PAX-5, and PIM-1 in thyroid lymphomas and chronic lymphocytic thyroiditis.

Patients	Age (y)/sex	Histology	c-MYC exon 1 and 2	RohH/TTF	PIM-1	PAX-5
Malignant lymphoma						
F1	73F	FL	T2501A, C2510T, G2529A, G2588A, G2611C, G2615T A2684G, A2695C, A2742G, G2777T, A2825C, T2853G G2866C, C2887T, T2913C, C2934A, T2976C, C2984G C2991G, C2993T, T2999C, C3065G, G3073A, G3089A C3158A, C3186G, T3191C, C3267G, C3331T, (C4807G)	G368T	G2497GA	–
F2	48F	FL	–	C448T	–	–
F3	54F	FL	A3045G	–	–	–
F4	59F	FL	G3035T	A460G	–	–
F5	60F	FL	(G5213A)	–	A2634T	–
F6	71F	FL	(T5236C)	–	G2050A	–
F7	50F	FL	G3035T	A1021T, del 701–1004	–	–
F8	66F	FL	(T4465C)	–	G2715A	–
F9	69F	FL	–	C838T	–	G812T
F11	67F	FL	–	G351C, A642C	–	–
F12	79M	FL	–	G698C, T710C	del2425–27	–
M1	76F	MZBCL	–	–	–	–
M2	65M	MZBCL	–	–	–	–
M3	73F	MZBCL	–	–	–	–
M4	67M	MZBCL	–	–	–	–
M5	70F	MZBCL	–	–	–	–
M6	73M	MZBCL	(G5213A)	–	–	–
M7	72F	MZBCL	–	–	–	–
M8	56F	MZBCL	–	–	–	–
M9	85F	MZBCL	–	–	–	–
M10	66M	MZBCL	–	–	–	–
D1	45F	DLBCL	G3035T	–	–	–
D2	61F	DLBCL	–	–	–	–
D3	67M	DLBCL*	–	–	–	–
D4	89F	DLBCL	C2879T, 3439del 8 bp	–	–	C1000T
D5	80F	DLBCL	–	–	–	–
D6	27F	DLBCL	–	–	–	–
D7	71F	DLBCL	–	–	–	–
D8	68F	DLBCL	–	–	–	–
D11	60F	DLBCL*	(C4498G)	–	C2757A	–
D12	60F	DLBCL	–	–	–	–
D13	81M	DLBCL*	–		–	–
D14	74F	DLBCL	–	–	A2634G	–
Chronic lymphocytic thyroiditis						
H1	50F		–	T420C	–	–
H2	57F		–	–	–	–
H3	55F		–	–	–	–
H4	67F		–	–	–	–
H5	66F		–	–	–	–
H6	61F		–	–	–	–
H7	68F		(T5338C)	–	–	–
H8	70F		–	–	–	–
H9	75F		–	–	–	–
H11	66F		–	–	–	–
H12	52F		–	–	–	–
H13	66M		–	–	–	–
H14	45F		–	–	–	–
H15	75F		–	–	–	–

FL, follicular lymphoma; DLBCL, diffuse large B-cell lymphoma; MZBCL, marginal zone B-cell lymphoma; *, germinal center B-cell-like phenotype.
Numbered according to GenBank accession numbers X00364 (c-MYC), AF386789 (RhoH/TTF), AF386792 (PIM-1), and AF386791 (PAX-5).
del, deletion; mutation located in exon 2 of c-MYC was shown in parenthesis.

Table 3
Summary of PIM-1, PAX-5, RhoH/TTF, c-MYC and BCL-6 mutations in thyroid lymphomas and chronic lymphocytic thyroiditis.

Gene	Mutation frequency/1000 bp		Insertion/deletion		Single bp substitution		Transitions/Transversions		G+C/A+T		RGYW	
	CLTH	TL	CLTH	TL	CLTH	TL	CLTH	TL	CLTH	TL	CLTH	TL
c-MYC												
exon1	0	4.35 (0.77–22.27)	0/0	0/1	0	34	0/0	16/18	0/0	23/11	0	14 (*p = 0.023)
exon2	0.86	0.86	0/0	0/0	1	6	1/0	4/2	0/1	4/2	0	1
RHOH/TTF	1.13	1.46 (1.13–2.26)	0/0	0/1	1	9	1/0	4/5	0/1	5/4	0	0
PIM-1	0	0.98	0/0	0/1	0	7	0/0	4/2	0/0	4/2	0	3
PAX-5	0	1.1	0/0	0/0	0	2	0/0	1/1	0/0	2/0	0	2
All genes	NA	NA	0/0	0/3	2	58	2/0	29/28	0/2	38/19	0	20
BCL-6	2.71 (1.35–4.06)	8.38 (1.35–20.30)	0/0	0/6	4	130	4/0	59/81	0/4	63/67	1	32 (*p = 0.033)

CLTH, chronic lymphocytic thyroiditis; TL, thyroid lymphoma.
* Significant by Chi-square test.

of 10 in MZBCL (50.0%) (Tables 1 and 4). Frequency of mutations was not significantly different between GC (2 of 3 (66.7%)) and non-GC (7 of 9 (77.8%)) subtypes in DLBCL. Mutation frequency for ASHM in *PAX-5* (1.1/1000 bp), *c-MYC exon 1* (1.1/1000 bp), *c-MYC exon 2* (0.86/1000 bp), *PIM-1* (0.98/1000 bp), and *RhoH/TTF* (0.98/1000 bp) was generally lower than that for SHM in BCL-6 sequences (8.38/1000 bp) in TL. Of the 130 single base-pair substitutions identified in the 33 specimens, 59 were transitions and 81 transversions, with a transition-to-transversion ratio of 0.73 (expected 0.5, $p = 0.13$, Chi-square test; Table 3). Mutations predominantly involved the RGYW/WRCY motifs ($p = 0.03$) (Table 3).

3.4. Clonality analysis of PIM-1, PAX-5, RhoH/TTF, and c-MYC

To investigate whether ASHM in TL is ongoing, clonality analysis for estimation of intraclonal heterogeneity was performed in 10 TL, consisting of 7 FL (F1, F5, F7, F8, F9, F11, F12) and 3 DLBCL (D4, D11, D14) with mutations in PIM-1, PAX-5, or RhoH/TTF by direct sequencing. In all tumors analyzed, 1 or 2 predominant alleles recapitulated the mutations observed by direct sequencing of the PCR product, confirming their presence in the tumor (not shown). A intraclonal variants were found in 3 of 7 FL and 1 of 3 DLBCL.

For comparison, clonality analysis of *BCL-6* gene was performed in 9 TL including of 3 FL (F1, F8, F9), 3 MZBCL (M3, M5, M8) and 3 DLBCL (D1, D2, D11). Intraclonal variants were found in 2 of 3 FL, 2 of 3 MZBCL and 3 of 3 DLBCL, respectively. A large number of intraclonal variants were found in 5 of these cases (F1, F9, D2, D9, M3). These data indicate that ASHM activity may be ongoing in a fraction of FL and DLBCL.

3.5. AID and POL-eta expression

AID and *POL-eta* are cellular gene products playing central roles in the DNA-modifying processes during immunoglobulin gene class switch recombination and SHM [8,9]. Expression level of AID was significantly higher in TL than in CLTH (Fig. 1), but was various among cases with TL. Expression level of AID was highest in DLBCL, followed by MZBCL and FL in order. Expression level of AID in ASHM negative cases was higher than that in ASHM positive cases, but statistically not significant ($p = 0.092$). Expression level of POL-eta was almost similar between TL and in CLTH, ASHM negative and positive cases, and among each histological type (data not shown).

4. Discussion

Occurrence of ASHM is initially regarded as a characteristic feature for nodal DLBCL based on the observation in systemic B-cell lymphomas [3]. Subsequent study demonstrated that ASHM also occurred in extra-nodal DLBCL of specific category such as AIDS-related [4], central nerves system [5], and mediastinal diseases [6,7]. ASHM was also found in FL [9,11]. ASHM occurred in both MZBCL and extranodal DLBCL, and suggested a role of ASHM for transformation from MZBCL to DLBCL [10]. Taken together, ASHM is supposed to contribute to lymphomagenesis in GC B-cell origin through induction of genome wide genetic instability covering multiple loci even outside the Ig genes, including c-MYC, *RhoH/TTF*, *PAX-5* and *PIM-1* proto-oncogenes. In addition, ASHM may induce occurrence of chromosomal translocations because the process of SHM is intrinsically associated with DNA double-strand breaks [3].

This study on TL revealed another aspects of ASHM as summarized below. (1) Involvement of ASHM with *PIM-1*, *RhoH/TTF*, and *c-MYC* was not so frequent in DLBCL of TL (4 (33.3%) of 12 cases), as reported previously for DLBCL in the different settings, i.e., nine (90%) of ten primary central nervous system lymphomas [5], 17 (100%) of 17 with extranodal DLBCLs [10], 10 (55.6%) of 18 AIDS-DLBCLs [4], and 14 (73.7%) of 19 primary mediastinal DLBCL [6,7]. (2) Involvement of ASHM with *PIM-1*, *RhoH/TTF*, and *c-MYC* was not common in MZBCL. Frequency of ASHM in MZBCL was not significantly different from that in DLBCL, which contrasts to the findings reported in the previous study by Deutsch et al. [10], i.e., ASHM was

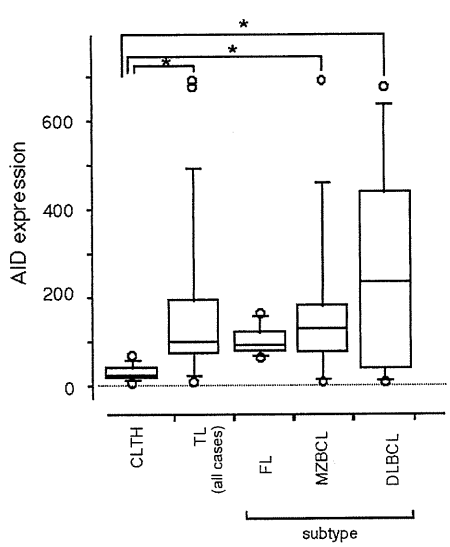

Fig. 1. *AID* expression in CLTH and ML. *AID* was expressed at significantly higher level in TL than in CLTH. Expression level of AID mRNA was highest in DLBCL, followed by MZBCL and FL.

Table 4
Mutational analysis of BCL-6 in thyroid lymohoma and chronic lymphocytic thiloiditis.

Patients	Age (y)/sex	Histology	BCL-6							
			Ins/del	Single bp substitution						
Thyroid lymphoma										
F1	73F	FL	–	G84C	T107G	C145G	T163G	G222C	T266A	C435T	C549T
				T557C	C566A	T569C	G647A	C656T			
F2	48F	FL	–	G66A	A80C	A99G	G132A	T181G	A191T	T194C	G322T
				G402C	C421A	T439C	T501G	G518A	C697T	T747A	
F3	54F	FL	–	–							
F4	59F	FL	–	G434A	G443A						
F5	60F	FL	–	–							
F6	71F	FL	–	T143C	G184C	G416T					
F7	50F	FL	–	–							
F8	66F	FL	del 132–478	C88G	A112G	T581G	T592C	G719C			
F9	69F	FL	–	G122C	G177C	A181G	G193A	T194C	G234A	C459G	T478A
F11	67F	FL	del 186–207	–							
F12	79M	FL	–	T247C	G347C						
M1	76F	MZBCL	–	–							
M2	65M	MZBCL	–	–							
M3	73F	MZBCL	–	G122C	C158T	T197G	C486G				
M4	67M	MZBCL	–	–							
M5	70F	MZBCL	del 173–418	T76C	C123T	C435T	G441C	C452G	T480G	C561T	A716G
M6	73M	MZBCL	–	A174G	T456A	C543A					
M7	72F	MZBCL	–	–							
M8	56F	MZBCL	del 90–454	T481A	T496C	C510T	G597A	T632A	T758C		
M9	85F	MZBCL	–	–							
M10	66M	MZBCL	del 429–534	A86T	G122A	G184A	A191C	A205T	T207C	C228G	A600G
				T645C	T687C	T745A					
D1	45F	DLBCL	del 97–479	T570G	T572A	G691T	A716G	A749T			
D2	61F	DLBCL	–	T89C	A99C	T107C	C123G	A191C	G369C	T517G	C544A
				T595C	T599A						
D3	67M	DLBCL*	–	C88T	T131A	G288C	A311T	T546C	T729C		
D4	89F	DLBCL	–	G294A	A344G	A506G					
D5	80F	DLBCL	–	G431A							
D6	27F	DLBCL	–	A72C	A90T	G184C	A205G	G211C	G229A	C490G	C519A
				C591G	C631A						
D7	71F	DLBCL	–	–							
D8	68F	DLBCL	–	T105A	C123G	A727G	G735C				
D11	60F	DLBCL*	–	T194C	C421A	T439C	T501G	G518A	C698T	T747A	
D12	60F	DLBCL	–	–							
D13	81M	DLBCL*	–	–							
D14	74F	DLBCL	–	T105A	G122C	T204G					
Chronic lymphocytic thiloiditis											
H1	50F		–	–							
H2	57F										
H3	55F		–	–							
H4	67F		–	–							
H5	66F		–	–							
H6	61F		–	–							
H7	68F		–	–							
H8	70F		–	T541C							
H9	75F		–	T600C	A645G	A710G					
H11	66F		–	–							
H12	52F		–	–							
H13	66M		–	–							
H14	45F		–	–							
H15	75F		–	–							

FL, follicular lymphoma; DLBCL, diffuse large B-cell lymphoma; MZBCL, marginal zone B-cell lymphoma; *, germinal center B-cell-like phenotype; del, deletion.
Numbered according to GenBank accession numbers AF191831 (BCL-6).

common in MZBCL (13 (76.5%) of 17 cases) but was much higher in DLBCL. They include lymphoma of various origins, such as stomach, orbita parotid gland, soft tissue and several thyroids. In our study, samples were derived from only thyroid using snap-frozen tissue. Libra et al. [8] reported that ASHM may not contribute significantly to both HCV-associated DLBCL and MZBCL. It is possible that the contribution of ASHM to lymphomagenesis in DLBCL and MZBCL may differ among the sites and the underlying disease derived from. (3) Involvement of ASHM with *PIM-1*, *RhoH/TTF*, and c-*MYC* was common in FL of TL (all of 11 cases), which was significantly higher than that in other kinds of TL ($p < 0.05$). Furthermore, the mutations found in c-MYC and PIM-1 in 2 cases of FL supposed to cause amino acid change. Whereas, involvement of ASHM with nodal FL was rare in the original report by Pasqualucci et al. [3], and it was found in 10 (53%) of 19 primary cutaneous FL [9] and 75–77% of FL [11]. (4) FL of thyroid was also unique in its lower level of AID expression compare to DLBCL and MZBCL. Expression level of AID gene was not correlated with the frequency of ASHM in the present series which is in consistent with the previous report [27].

ASHM has so far never been described in non-lymphoma tissues. It is somewhat unexpected that ASHM was found in a fraction of CLTH. We have confirmed the reactive and non-neoplastic nature of CLTH lesions by clonality assays [24,26]. There are at least three possible explanations for this discrepancy. The first is that ASHM

may really occur in CLTH. The second is that the nucleotide change may result from polymorphysm but not ASHM. The other possibility is that the lesions are mixture of CLTH and lymphoma that has just arisen from the CLTH. Further analysis may be necessary for discriminating these possibilities.

TL is one of well-known type of lymphomas developing in mucosa-associated lymphoid tissue, but information for molecular genetic features of TL was quite limited until present. Present data provide an insight about the oncogenesis of TL, i.e., ASHM may play a role in the development of FL, while not so much in MZBCL. DLBCL consists of ASHM negative and positive cases, indicating the heterogeneous character of this lymphoma. ASHM negative DLBCL cases may be derived from a MZBCL/DLBCL axis or de novo and not from the transformed FL. As for ASHM positive DLBCL, three possibilities must be taken into account: the first is transformation of FL to DLBCL, the second is increase of ASHM during transformation of MZBCL to DLBCL, and the third is DLBCL arising de novo.

Conflict of interest

None.

Acknowledgement

Supported by grants from the Ministry of Education, Science, Culture, and Sports, Japan (14031213, 14770073, 15026209, 15406013, 15590340, 16390105, 18014015).

References

[1] Kuppers R, Klein U, Hansmann ML, Rajewsky K. Cellular origin of human B-cell lymphomas. N Engl J Med 1999;341:1520–9.
[2] Shen HM, Peters A, Baron B, Zhu X, Storb U. Mutation of BCL-6 gene in normal B cells by the process of somatic hypermutation of Ig genes. Science 1998;280:1750–2.
[3] Pasqualucci L, Neumeister P, Goossens T, Nanjangud G, Chaganti RS, Kuppers R, et al. Hypermutation of multiple proto-oncogenes in B-cell diffuse large-cell lymphomas. Nature 2001;412:341–6.
[4] Gaidano G, Pasqualucci L, Capello D, Berra E, Deambrogi C, Rossi D, et al. Aberrant somatic hypermutation in multiple subtypes of AIDS-associated non-Hodgkin lymphoma. Blood 2003;102:1833–41.
[5] Montesinos-Rongen M, Van Roost D, Schaller C, Wiestler OD, Deckert M. Primary diffuse large B-cell lymphomas of the central nervous system are targeted by aberrant somatic hypermutation. Blood 2004;103:1869–75.
[6] Bödör C, Bognár A, Reiniger L, Szepesi A, Tóth E, Kopper L, et al. Aberrant somatic hypermutation and expression of activation-induced cytidine deaminase mRNA in mediastinal large B-cell lymphoma. Br J Hematol 2005;129:373–6.
[7] Rossi D, Cerri M, Capello D, Deambrogi C, Berra E, Franceschetti S, et al. Aberrant somatic hypermutation in primary mediastinal large B-cell lymphoma. Leukemia 2005;19:2363–6.
[8] Libra M, Capello D, Gloghini A, Laura P, Berra E, Cerri M, et al. Analysis of aberrant somatic hypermutation (SHM) in non-Hodgkin's lymphomas of patients with chronic HCV infection. J Pathol 2005;206:87–91.
[9] Dijkman R, Tensen CP, Buettner M, Niedobitek G, Willemze R, Vermeer MH. Primary cutaneous follicle center lymphoma and primary cutaneous large B-cell lymphoma, leg type, are both targeted by aberrant somatic hypermutation but demonstrate differential expression of AID. Blood 2006;107:4926–9.
[10] Deutsch AJ, Aigelsreiter A, Staber PB, Beham A, Linkesch W, Guelly C, et al. MALT lymphoma and extranodal diffuse large B-cell lymphoma are targeted by aberrant somatic hypermutation. Blood 2007;109:3500–4.
[11] Halldórsdóttir AM, Frühwirth M, Deutsch A, Aigelsreiter A, Beham-Schmid C, Agnarsson BA, et al. Quantifying the role of aberrant somatic hypermutation in transformation of follicular lymphoma. Leuk Res 2008;32:1015–21.
[12] Freeman C, Berg JW, Cutler SJ. Occurrence and prognosis of extranodal lymphomas. Cancer 1972;29:252–60.
[13] Aozasa K, Tsujimoto M, Sakurai M, Honda M, Yamashita K, Hanada M, et al. Non-Hodgkin's lymphomas in Osaka. Japan Eur J Cancer Clin Oncol 1985;21:487–92.
[14] Volpe R. Thyroiditis: current views of pathogenesis. Med Clin North Am 1975;59:1163–75.
[15] Kato I, Tajima K, Suchi T, Aozasa K, Matsuzuka F, Kuma K, et al. Chronic thyroiditis as a risk factor of B-cell lymphoma in the thyroid gland. Jpn J Cancer Res (Gann) 1985;76:1085–90.
[16] Jaffe ES, Harris NL, Stein H, Vardiman JW. World Health Organization classification of tumours pathology and genetics of tumours of haematopoietic and lymphoid tissues. Lyon: IARC Press; 2001.
[17] Miwa H, Takakuwa T, Nakatsuka S, Tomita Y, Matsuzuka F, Aozasa K. DNA sequence of immunoglobulin heavy chain variable region gene in thyroid lymphoma. Jpn J Cancer Res 2001;92:1041–7.
[18] Sato Y, Nakamura N, Nakamura S, Sakugawa S, Ichimura K, Tanaka T, et al. Deviated VH4 immunoglobulin gene usage is found among thyroid mucosa-associated lymphoid tissue lymphomas, similar to the usage at other sites, but is not found in thyroid diffuse large B-cell lymphomas. Mod Pathol 2006;19:1578–84.
[19] Goodman MF. Error-prone repair DNA polymerases in prokaryotes and eukaryotes. Annu Rev Biochem 2002;71:17–50.
[20] Muramatsu M, Kinoshita K, Fagarasan S, Yamada S, Shinkai Y, Honjo T. Class switch recombination and hypermutation require activation-induced cytidine deaminase (AID), a potential RNA editing enzyme. Cell 2000;102:553–63.
[21] Petersen-Mahrt SK, Harris RS, Neuberger MS. AID mutates *E. coli* suggesting a DNA deamination mechanism for antibody diversification. Nature 2002;418:99–103.
[22] Zeng X, Winter DB, Kasmer C, Kraemer KH, Lehmann AR, Gearhart PJ. DNA polymerase eta is an A-T mutator in somatic hypermutation of immunoglobulin variable genes. Nat Immunol 2001;2:537–41.
[23] Hans CP, Weisenburger DD, Greiner TC, Gascoyne RD, Delabie J, Ott G, et al. Confirmation of the molecular classification of diffuse large B-cell lymphoma by immunohistochemistry using a tissue microarray. Blood 2004;103:275–82.
[24] van Dongen JJ, Langerak AW, Bruggemann M, Evans PA, Hummel M, Lavender FL, et al. Design and standardization of PCR primers and protocols for detection of clonal immunoglobulin and T-cell receptor gene recombinations in suspect lymphoproliferations: report of the BIOMED-2 Concerted Action BMH4-CT98-3936. Leukemia 2003;17:2257–317.
[25] D'Haese JG, Tsukasaki K, Cremer FW, Fischer C, Bartram CR, Jauch A. Chromosomal aberrations in follicular non-Hodgkin lymphomas of Japanese patients, detected with comparative genomic hybridization and polymerase chain reaction analysis. Cancer Genet Cytogenet 2005;162:107–14.
[26] Yamauchi A, Tomita Y, Takakuwa T, Hoshida Y, Nakatsuka S, Sakamoto H, et al. Polymerase chain reaction-based clonality analysis in thyroid lymphoma. Int J Mol Med 2002;10:113–7.
[27] Pasqualucci L, Guglielmino R, Houldsworth J, Mohr J, Aoufouchi S, Polakiewicz R, et al. Expression of the AID protein in normal and neoplastic B cells. Blood 2004;104:3318–25.

Int. J. Cancer: **125**, 381–387 (2009)

WT1 IgG antibody for early detection of nonsmall cell lung cancer and as its prognostic factor

Yusuke Oji[1], Yayoi Kitamura[1], Eriko Kamino[2], Aiko Kitano[1], Noriyoshi Sawabata[3], Masayoshi Inoue[4], Masahide Mori[5], Shin-ichi Nakatsuka[6], Nao Sakaguchi[2], Kaori Miyazaki[2], Michiyo Nakamura[2], Ikuyo Fukuda[2], Junya Nakamura[2], Naoya Tatsumi[2], Tetsuya Takakuwa[7], Sumiyuki Nishida[8], Toshiaki Shirakata[1], Naoki Hosen[9], Akihiro Tsuboi[8], Riichiro Nezu[10], Hajime Maeda[11], Yoshihiro Oka[12], Ichiro Kawase[12], Katsuyuki Aozasa[7], Meinoshin Okumura[4], Shinichiro Miyoshi[3] and Haruo Sugiyama[2]*

[1]*Department of Biomedical Informatics, Osaka University Graduate School of Medicine, Suita, Osaka, Japan*
[2]*Department of Functional Diagnostic Science, Osaka University Graduate School of Medicine, Suita, Osaka, Japan*
[3]*Department of Cardiothoracic Surgery, Dokkyo Medical University, Tsuga-gun, Tochigi, Japan*
[4]*Department of Thoracic Surgery, Osaka University Graduate School of Medicine Suita, Osaka, Japan*
[5]*Department of Respiratory Medicine, Toneyama National Hospital, Toyonaka, Osaka, Japan*
[6]*Department of Pathology, Sumitomo Hospital, Osaka, Osaka, Japan*
[7]*Department of Pathology, Osaka University Graduate School of Medicine, Suita, Osaka, Japan*
[8]*Department of Cancer Immunotherapy, Osaka University Graduate School of Medicine, Suita, Osaka, Japan*
[9]*Department of Cancer Stem Cell Biology, Osaka University Graduate School of Medicine, Suita, Osaka, Japan*
[10]*Department of Surgery, Osaka Rosai Hospital, Sakai, Osaka, Japan*
[11]*Department of Thoracic Surgery, Toneyama National Hospital, Toyonaka, Osaka, Japan*
[12]*Department of Respiratory Medicine and Allergy, Rheumatic Disease, Osaka University Graduate School of Medicine, Suita, Osaka, Japan*

There are urgent needs to develop methods for early detection of nonsmall cell lung cancer (NSCLC) because of its increasing incidence and poor prognosis. Here, we analyzed the production of IgG antibody (WT1 Ab) against WT1 (Wilms' tumor gene) protein that was overexpressed in the majority of NSCLC. Enzyme-linked immuno-sorbent assay showed that WT1 Ab was produced in all of 91 NSCLC patients and 70 healthy individuals and that WT1 Ab titers were significantly higher in NSCLC patients compared with healthy individuals. When the cut-off level of WT1 Ab titers were fixed at mean + 3SD of those in healthy individuals, 26.4% of NSCLC patients had WT1 Ab titers over the cut-off level, and positive rates of WT1 Ab at each clinical stage were 25.0, 30.8 and 38.4% in stage I, II and III NSCLC, respectively. When WT1 Ab was combined with CEA or CYFRA for detection of NSCLC, positive detection rates increased from 25.0 to 34.1 and 31.8%, respectively, in stage I and from 38.4 to 69.2 and 46.1%, respectively, in stage III, but not changed in stage II. Western blot analysis showed that dominant subclass of WT1 Ab was Th1-type IgG2. Interestingly, elevation of WT1 Ab titers was significantly associated with longer disease-free survival in patients with stages I–III NSCLC. These results showed that WT1 Ab could be a useful marker for early detection of NSCLC and its prognostic prediction. These results also suggested that WT1-specific immune responses played an important role in anti-cancer immunity in NSCLC.

Key words: lung cancer; WT1; humoral immune response; tumor marker; prognostic marker

Lung cancer is the leading cause of cancer death in the world and nonsmall cell lung cancer (NSCLC) represents nearly 80% of the disease.[1] Because 75% of lung cancer patients are diagnosed at stages of metastatic spread when therapies are rarely curative,[2] early detection of localized lung cancer is the key to improve its clinical outcome.

Although chest X-ray is routinely used as a screening tool, its limitation to detect localized lung cancer has been evident because of its insufficient sensitivity.[2] Recently, low-dose spiral computed tomography (CT) has been proposed as an early detection screening tool. However, despite its high sensitivity, specificity of CT in lung cancer detection is poor.[3] Therefore, serum biomarkers with high sensitivity and specificity for diagnosis of lung cancer are needed. However, current serum biomarkers for NSCLC such as carcino embryonic antigens (CEA) and squamous cell carcinoma antigen do not have sufficient sensitivity and specificity required for early detection of NSCLC.[4,5]

It is now clear that malignant transformation occurs by changes in cellular gene expression with subsequent clonal proliferation. Altered gene expression in malignant cells may lead to the expression of aberrantly expressed proteins recognized by host immune system. If autoantibodies against these antigens are produced at early stage of NSCLC when quantity of the tumor antigens in the circulation is very small, these antibodies should be useful markers for early detection of NSCLC. Moreover, because production of IgG antibodies needs helper T-cell functions and helper T cells play an important role in cellular immune responses, IgG antibodies against tumor antigens may be more useful markers for predicting prognosis in NSCLC patients compared with IgM antibodies.

The *WT1* gene was originally isolated as a tumor suppressor gene responsible for a kidney neoplasm of the childhood, Wilms' tumor.[6] However, we have demonstrated that the wild-type *WT1* gene is overexpressed in leukemia[7] and various types of solid cancers including lung,[8,9] gastric,[10] esophageal,[11] colorectal[12] and pancreatic cancers.[13] We proposed that the wild-type *WT1* gene played oncogenic roles rather than tumor-suppressor functions in tumorigenesis of various types of cancers.[14–16] We had previously demonstrated that IgG and IgM Ab against WT1 were produced at higher levels in patients with AML and MDS compared with normal individuals[17] and that Th1 type subclasses of WT1 IgG Ab, IgG1, 2, and 3 were dominantly produced in the patients.[18] On the other hand, production of WT1 Ab in patients with solid tumors remained undetermined.

In the present study, we demonstrate that high titers of Th1 type WT1 IgG antibody are detected in 26.4% of NSCLC patients and positive detection rate of WT1 Ab was higher than that of CEA or CYFRA in stages I and II NSCLC. Moreover, we describe that

Grant sponsor: Ministry of Education, Science, Sports, Culture and Technology and the Ministry of Health, Labour, and Welfare, Japan.
***Correspondence to:** Department of Functional Diagnostic Science, Osaka University Graduate School of Medicine, 1-7 Yamada-Oka, Suita, Osaka, Japan. Fax: +81-6-6879-2597.
E-mail: sugiyama@sahs.med.osaka-u.ac.jp
Received 25 December 2008; Accepted after revision 3 February 2009
DOI 10.1002/ijc.24367
Published online 18 February 2009 in Wiley InterScience (www.interscience.wiley.com).

TABLE I – CHARACTERISTICS OF THE PATIENTS WITH NSCLC

	Stage				Age (median)	Sex (M:F)	Total
	I	II	III	Unknown			
Adenocarcinoma	27	5	9	13	42–83 (70)	32:22	54
Squamous Cell Carcinoma	13	6	1	9	48–85 (68)	23:6	29
Large Cell Carcinoma	4	0	0	0	63–81 (72)	4:0	4
Pleomorphic Carcinoma	1	0	1	0	60–82	2:0	2
Adeno-squamous Cell Carcinoma	0	1	1	0	74–75	1:1	2

high titers of WT1 IgG Ab are associated with longer disease-free survival (DFS) in stages I–III NSCLC.

Material and methods

Serum samples

Serum samples were obtained from 91 patients with nonsmall cell lung cancer (54 adenocarcinoma, 29 squamous cell carcinoma, 4 large cell carcinoma, 2 pleomorphic carcinoma, 2 adenosquamous cell carcinoma) before operation and from 70 healthy individuals under written informed consent at Dokkyo Medical University Hospital, Toneyama National Hospital, Osaka Rosai Hospital and Osaka University Hospital. Characteristics of the patients are shown in Table I. The samples were stocked at −80°C until use.

Tissue samples

Tissue samples were obtained from 41 patients (40 adenocarcinoma and 1 squamous cell carcinoma) with stage I NSCLC at Osaka University Hospital under informed consent.

Construction of vectors for recombinant WT1 protein

To obtain recombinant full length WT1 protein and one each of three WT1 fragment proteins [WT-Fr1 (1–182aa), WT-Fr2 (180–324aa) and WT-Fr3 (318–449 aa)], corresponding region of the *WT1* gene was amplified by PCR using Pfx polymerase (Invitrogen, Carlsbad, CA) and inserted into the pGEX-5X-3 vector (GE Healthcare Biosciences, Piscataway, NJ) that allowed the expression of the recombinant protein with an N-terminal GST tag. GST tagged, full length WT1 protein was purified by size fractionation using NA-1800 apparatus (Nippon Eido, Tokyo, Japan) according to the manufacturer's instructions. WT1 fragment proteins and GST protein were purified using Glutathione Sepharose 4 Fast Flow beads (GE Healthcare Biosciences) according to the manufacturer's instructions.

Enzyme-linked immunosorbent assay

Enzyme-linked immunosorbent assay (ELISA) was established to measure the titers of WT1 IgG Ab present in serum from patients and healthy individuals. ELISA 96 well plates (Multi Well Plate H Type Plate MS-8896F, Sumitomo Bakelite, Japan) were coated with 100 μl of recombinant GST tagged, full length WT1 protein (20 μg/ml) in immobilization Buffer (10 mM $NaCO_3$, 30 mM $NaHCO_3$, 0.02% NaN_3, pH 9.6 overnight at 37°C. Plates were washed with Tris-buffered saline (TBS) and blocked with Blocking solution (TBS containing 0.05% Tween20 and 1% gelatin) at 37°C for 2 hr. Sera were diluted at 1:1,600 in Blocking solution and pre-absorbed by immobilized GST protein at 4°C overnight. Then, 100 μl of the diluted sera was added to each well for overnight incubation at 4°C. Plates were washed with TBST (TBS containing 0.05% Tween20) and incubated with ALP-conjugated goat anti-human IgG Ab (Santa Cruz Biotechnology, CA) diluted at 1:1,000 in TBST (TBS containing 1% Tween20) for 2 hr at room temperature. After washing, bound WT1 IgG Ab was visualized using 50 μl of BCIP/NBT kit (Nacalai Tesque, Kyoto, Japan) for each well. Then, absorbance at 550 nm was measured using a microplate reader MTP-32 (Corona Electric, Ibaraki, Japan). All sera were examined in duplicate. The titers of WT1 IgG Ab were calculated by interpolation from the standard line which was constructed for each assay from the results of simultaneous ELISA assay using serial diluted WT1 6F-H2 Ab using ALP-conjugated goat anti-mouse IgG Ab (diluted at 1:1,000; Santa Cruz Biotechnology) as the second Ab. WT1 Ab titers in the sera that produced the absorbance at 550 nm equal to that produced by 0.1 μg/ml of WT1 monoclonal 6F-H2 (Dako Cytomation, Golstrup, Denmark) Ab was defined as a 1.0 WT1-reacting-unit (WRU) in the ELISA system. Thus, WT1 IgG Ab titers of sera were measured to be [(concentrations of 6F-H2 mAb (μg/ml) corresponding to the absorbance at 550 nm produced by the diluted sera on the standard line) × (ratio of serum dilution) × 10] WRU. When titers of WT1 IgG Ab were high and out of measurable range in the ELISA system, the sera were diluted with Blocking solution to measurable levels and reanalyzed to determine the titers of WT1 IgG Ab.

Western blot analysis

For detection of WT1 IgG Ab, sera were diluted at 1:1,000, reacted with immobilized recombinant GST protein (200 ng) at 4°C overnight, and then reacted at room temperature overnight with GST tagged, full length WT1 protein or one each of three WT1 fragment proteins (200 ng) that was transferred onto PVDF membrane after SDS-PAGE. WT1 IgG Ab captured by the protein was visualized by ALP-conjugated anti-human IgG Ab or ALP-conjugated anti-human IgG subclass-specific Ab using a BCIP/NBT kit (Nacalai Tesque).

For analysis of relative amount of subclasses of WT1 IgG Ab and total IgG, 5 μl of diluted serum (diluted at 1:10 with 2 × Laemieli's SDS sample buffer) were loaded onto SDS-PAGE gel and the serum proteins were transferred onto PVDF membrane. Then, the membrane was reacted with ALP-conjugated anti-human IgG subclass-specific Ab at room temperature overnight and the bound Ab was visualized by using a BCIP/NBT kit.

ALP-conjugated anti-human IgG Ab was purchased from Santa Cruz Biotechnology and used at the dilution of 1:1,000. ALP-conjugated anti-human IgG1 (#05-3322), IgG2 (#05-3522), IgG3 (#05-3622) and IgG4 (#05-3822) Ab were purchased from Zymed Laboratories (San Francisco, CA) and used at the dilution of 1:500. WT1 monoclonal 6F-H2 antibody against 180aa residues in the amino terminal region of WT1 protein (Dako Cytomation), WT1 polyclonal C-19 antibody against 19aa residues near the carboxy terminus of WT1 protein (Santa Cruz Biotechnology) and GST antibody (Santa Cruz Biotechnology) were used as a first antibody. WT1 IgG Ab detected in Western blot analysis was scored into three categories; positive (WT1 IgG Ab was detected as a band with strong or intermediate density), weakly positive (WT1 IgG Ab was detected as a band with weak density), and negative (WT1 IgG Ab was not detected).

Immunohistochemistry

Formalin-fixed tissue sections of 3-μm thickness were cut from each paraffin-block. After dewaxing with xylene and rehydration through a graded series of ethanol, the sections were antigen retrieved using Pascal apparatus (Dako Cytomation) in 10 mM citrate buffer (pH 6.0). These sections were reacted with WT1 C-19 Ab (diluted at 1:100, Santa Cruz Biotechnology) at 4°C overnight and then reacted with Envision kit/HRP (Dako Cytomation) at room temperature for 30 min. After treatment with 0.7% H_2O_2 so-

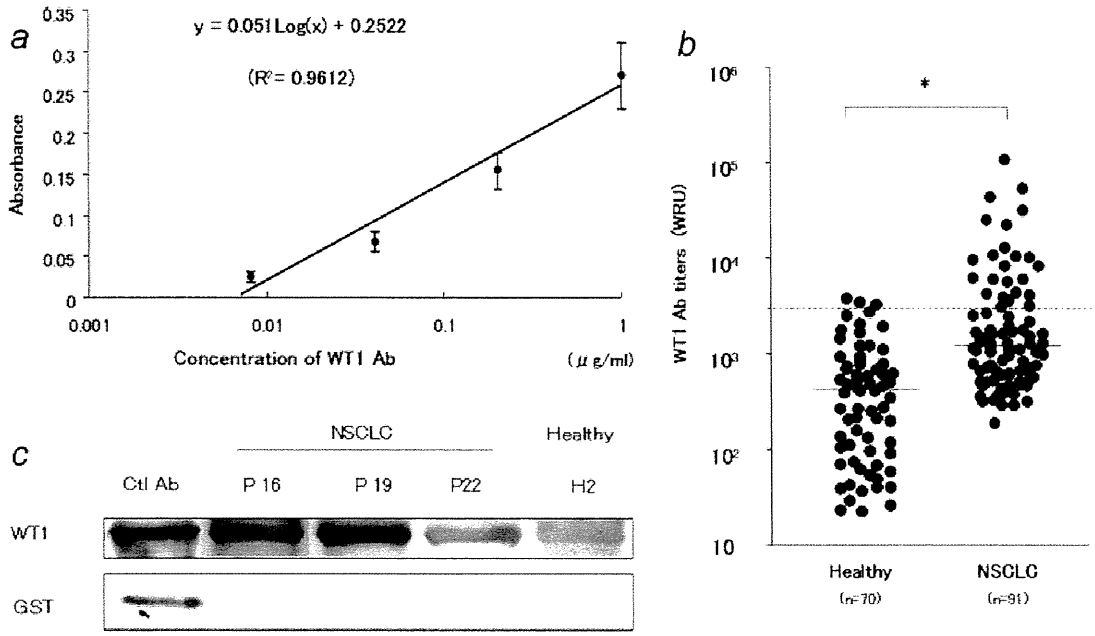

FIGURE 1 – Enhanced production of WT1 IgG Ab in NSCLC patients. (*a*) A representative standard line of the ELISA system for measurement of the titers of WT1 IgG Ab. The absorbance at 550 nm produced by serial dilution of WT1 monoclonal 6F-H2 Ab was measured by the ELISA system. The results are from four independent assays, and the mean ± SE is shown. WT1 Ab titer that produces the absorbance at 550 nm equal to that produced by 0.1 μg/ml of WT1 monoclonal 6F-H2 Ab in the ELISA system was defined as 1.0 WT1-reacting-unit (WRU). (*b*) Increased WT1 Ab titers in NSCLC patients. WT1 Ab titers were examined by the ELISA system in 91 NSCLC patients and 70 healthy individuals. Dotted line shows the cut-off level (2,910 WRU) of WT1 Ab titers, $*p < 0.05$. (*c*) Detection of WT1 IgG Ab by Western blot analysis in NSCLC patients. Western blot analysis was performed as described in "Material and Methods". As representative results, those from three NSCLC patients (P16, P19 and P22) and healthy individual (H2) are shown. WT1 monoclonal 6F-H2 Ab and GST Ab were used to show the positions of GST-WT1 protein and GST protein, respectively.

lution to reduce endogenous peroxidase activity, immunoreactive WT1 protein was visualized using DAB tablet (Wako, Osaka, Japan). The sections were then counterstained with hematoxylin.

Statistical analysis

The Welch's *t* test was used to calculate the difference between the titers of WT1 IgG Ab of NSCLC patients and those of healthy individuals. Statistical analysis for correlations between the titers of WT1 IgG Ab and the clinical parameters and was performed using Welch's *t* test or Kruskal–Wallis test. Statistical analysis for prognosis between NSCLC patients with or without elevated WT1 IgG Ab titers was performed by log-rank's test.

Results

Establishment of ELISA system for measurement of WT1 IgG Ab

Enzyme-linked immunosorbent assay (ELISA) system was established to measure the titers of WT1 IgG Ab (WT1 Ab titers) in the sera from NSCLC patients and healthy individuals. In the ELISA system, WT1 IgG Ab was captured by GST tagged, full length WT1 protein and visualized using ALP-conjugated anti-human IgG Ab. WT1 Ab titers were calculated by interpolation from the standard line, which was constructed from the results of simultaneous ELISA assay using serial diluted WT1 monoclonal 6F-H2 Ab. The absorbance at 550 nm produced by serially diluted WT1 monoclonal 6F-H2 Ab showed a linear plot ($R^2 = 0.9612$) against the concentrations of 6F-H2 Ab ranging from 0.008 to 1 μg/ml (Fig. 1*a*). WT1 Ab titers in the sera that produced the absorbance at 550 nm equal to that produced by 0.1 μg/ml of WT1 monoclonal 6F-H2 Ab was defined as a 1.0 WRU. Thus, WT1 IgG Ab titers of sera were measured to be [(concentrations of 6F-H2 mAb (μg/ml) corresponding to the absorbance at 550 nm produced by the diluted sera on the standard line) × (ratio of serum dilution) × 10] WRU. The standard line was reproducible with between-run coefficient of variation (CV) of 7.5% in 10 independent assays.

Elevation of WT1 IgG Ab in NSCLC patients

WT1 Ab titers (WRU) were examined in 91 NSCLC patients and 70 healthy individuals. WT1 IgG Ab was detected in all the samples examined (Fig. 1*b*). WT1 Ab titers ranged from 10 to 3,664 (median 392) and from 183 to 104,940 (median 1,135) WRU in healthy individuals and NSCLC patients, respectively. Therefore, WT1 Ab titers were significantly ($p < 0.05$) higher in NSCLC patients than in healthy individuals. When the cut-off level of WT1 Ab titers was fixed at 2,910 WRU, which was mean + 3SD of WT1 Ab titers in healthy individuals, 24 (26.4%) of 91 NSCLC patients had WT1 Ab over the cut-off level.

To confirm the presence of WT1 IgG Ab in sera from NSCLC patients and healthy individuals, sera of randomly selected 31 NSCLC patients and 27 healthy individuals were reacted with immobilized recombinant GST protein and then examined for WT1 IgG Ab by Western blot analysis using GST-WT1 protein as an antigen. WT1 IgG Ab was detected in all of the 31 NSCLC patients and 27 healthy individuals examined (Fig. 1*c*, upper panels). Furthermore, to confirm that the bands detected did not result from the reaction of GST portion of GST-WT1 protein with antibodies against GST in the patients' sera, Western blot analysis was performed using the sera which was pre-reacted with immobilized GST protein and purified GST protein as an antigen. As expected, sera of the patients and healthy individuals did not react with GST protein (Fig. 1*c*, lower panels). These results showed that Western blot analysis used here could specifically detect WT1 IgG Ab.

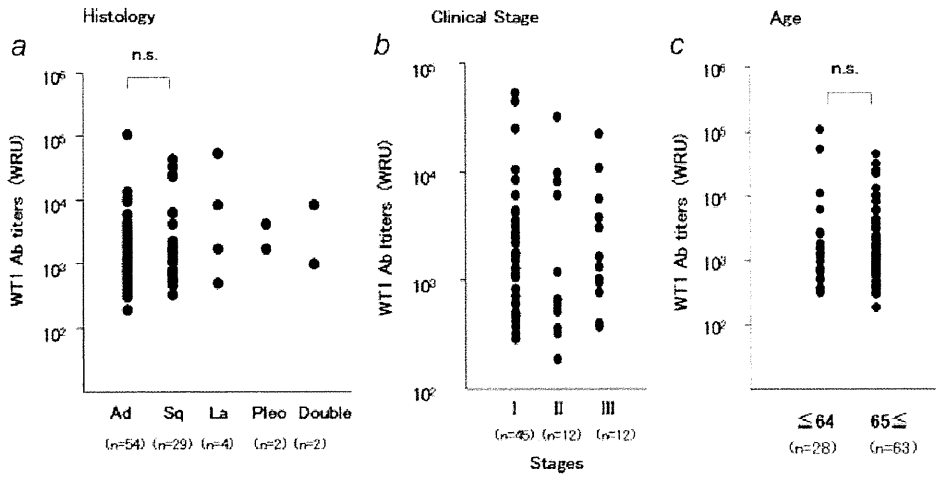

FIGURE 2 – No correlation between WT1 Ab titers and clinical parameters of NSCLC. Correlations between WT1 Ab titers and clinical parameters of NSCLC, histology (*a*), clinical stages (*b*) and age (*c*) are shown. n.s., Not significant.

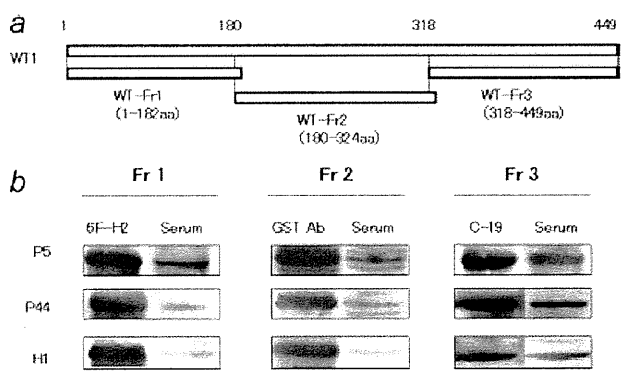

FIGURE 3 – Epitope distribution of WT1 IgG Ab. (*a*) Schema of WT1 fragment proteins. Recombinant WT1 fragment proteins were expressed in bacterial hosts. (*b*) Western blot analysis for epitope distribution of WT1 IgG Ab. Western blot analysis was performed. WT1 antibodies, 6F-H2 monoclonal Ab against 180 aa residues at the amino terminus of WT1 protein and C-19 polyclonal Ab against 19 aa residues near the carboxy terminus were used as positive control antibodies recognizing WT-Fr1 and WT-Fr3, respectively. Because WT1 antibody recognizing WT-Fr2 was not available, GST antibody was used to show the band responsible for WT-Fr2 with GST tag. Representative results of NSCLC patients (P5 and P44) and a healthy individual (H1) are shown.

No correlation between WT1 Ab titers and clinical parameters in NSCLC patients

Whether or not WT1 Ab titers were correlated with clinical parameters was examined in NSCLC patients. As shown in Figure 2, no correlation was found between WT1 Ab titers and clinical parameters such as histology, clinical stages and age.

Epitope distribution of WT1 IgG Ab in NSCLC patients and healthy individuals

Epitope distribution of WT1 IgG Ab was examined in the 31 NSCLC patients and 27 healthy individuals by Western blot analysis using three purified, recombinant WT1 fragment proteins, WT-Fr1 (1–182aa), WT-Fr2 (180–324aa) and WT-Fr3 (318–449aa) as antigens (Fig. 3*a*). Sera from 30 (96.8%) of 31 NSCLC patients and 24 (88.9%) of 27 healthy individuals examined recognized two or three WT1 fragment proteins (Fig. 3*b*). These results indicated the presence of multiple antigenic epitopes within WT1 protein.

Dominant subclass of WT1 IgG Ab is IgG2

To examine whether humoral immune responses against WT1 protein were Th1- or Th2- type, subclasses of WT1 IgG Ab against WT-Fr3 protein, which was recognized by all of the sera examined, were examined by Western blot analysis in the 31 NSCLC patients and the 27 healthy individuals (Fig. 4). IgG2 was a dominant subclass of WT1 Ab in all of the patients and healthy individuals examined (Fig. 4*a*, upper panels). To confirm that this IgG2 dominance did not result from the reflection of the dominance of total IgG2 subclass, subclasses of total IgG were simultaneously determined (Fig. 4*a*, lower panels). Differently from the IgG2 dominance of WT1 IgG Ab, the dominant subclass of total IgG was IgG1. These results showed that dominant subclass of WT1 IgG Ab was IgG2. In NSCLC patients, positivity (see "Material and Methods") of WT1 IgG1, IgG2, IgG3 and IgG4 subclass Ab were 22.6% (7 of 31), 64.5% (20 of 31), 19.4% (6 of 31) and 12.9% (4 of 31), respectively (Figs. 4*a*, 4*b*). In healthy individuals, positivity of WT1 IgG1, IgG2, IgG3 and IgG4 subclass Ab were 22.2% (6 of 27), 77.8% (21 of 27) , 29.6% (8 of 27) and 29.6% (8 of 27), respectively.

To confirm the semiquantitative nature of the Western blot analysis used here, it was performed by using WT-Fr3 protein as an antigen and serially diluted serum from a NSCLC patient (P4). As shown in Fig. 4*c*, the band density of IgG2 WT1 Ab, which was dominantly contained in the serum, decreased as the serum was diluted at the ratio of 1:200, 1:600 and 1:1,800, confirming that the Western blot analysis used here could semi-quantitatively detect WT1 IgG Ab.

Therefore, production of Th1-type, IgG2 WT1 Ab was enhanced in NSCLC patients, indicating that Th1-type humoral immune responses against WT1 protein were elicited in NSCLC patients.

WT1 Ab as a biomarker for detection of NSCLC

Positivity of WT1 Ab was compared with that of currently available tumor markers, CEA and CYFRA, in NSCLC patients. Clinical data of CEA and CYFRA were available for 70 (44 on stage I, 13 on stage II and 13 on stage III) and 59 patients (36 on stage I, 12 on stage II and 11 on stage III) with NSCLC, respectively. As shown in Figure 5, WT1 Ab titers did not correlate with serum levels of CEA (Fig. 5*a*) and CYFRA (Fig. 5*b*). Positive detection rate for WT1 Ab, CEA and CYFRA was 25.0 (11 of 44), 13.6 (6 of 44) and 11.1% (4 of 36) in stage I NSCLC patients; 30.8 (4 of 13), 23.1 (3 of 13) and 16.7% (2 of 12) in stage II patients and 38.5 (5 of 13), 46.2 (6 of 13) and 18.2% (2 of 11) in stage III patients, respectively (Fig. 5*c*). Because positive detec-

tion rate of WT1 Ab was 25.0%, which was higher than that of either CEA or CYFRA, in stage I NSCLC patients, it may be a useful marker for early detection of NSCLC.

When WT1 Ab was combined with CEA or CYFRA for detection of NSCLC, positive detection rates increased from 25.0 to 34.1 and 31.8%, respectively, in stage I and from 38.4 to 69.2 and 46.1%, respectively, in stage III, but not changed in stage II (Fig. 5*c*). Thus, WT1 Ab is useful for sensitive detection of NSCLC in combination with CEA or CYFRA.

Overexpression of WT1 protein in early stage NSCLC

To confirm the expression of WT1 protein in early stage NSCLC, the expression of WT1 protein was examined by immunohistochemistry in 41 patients with stage I NSCLC. WT1 expression in cancer cells was scored into the following three categories: positive, weakly positive and negative staining meant strong, slightly stronger and similar one of lung cancer cells, respectively, compared with that of the alveolar epithelial cells of lung. In positive or weakly positive cases, WT1 protein was dominantly detected in the cytoplasm of lung cancer cells. WT1 protein expression in lung cancer cells was positive in 30 (73.2%), weakly positive in 7 (17.1%), and negative in the remaining 4 (9.8%), of 41 NSCLC patients (Fig. 5*d*). Thus, WT1 protein was overexpressed in 90.3% (37 of 41) of stage I NSCLC patients examined.

Elevation of WT1 Ab is associated with favorable prognosis in NSCLC patients

To examine whether or not enhanced humoral immune responses against WT1 were associated with lower relapse rates in patients with NSCLC, DFS rates were analyzed between two groups of NSCLC patients whose follow-up data after surgery were available: 20 patients with elevated WT1 Ab titers (52,110–3,514; median 8,777 WRU) and 59 patients without elevated WT1 Ab titers (2,648–183; median 655 WRU). In patients with elevated WT1 Ab titers, 1-, 2- and 3-year DFS rates of the patients were 100, 94.7 and 94.7%, respectively. In contrast, in patients without elevated WT1 Ab titers, 1-, 2- and 3-year DFS rates were 88.0, 82.8 and 77.4%, respectively. Kaplan–Meier curve and log rank's test showed that patients with elevated WT1 Ab titers had significantly ($p = 0.002$) longer DFS than those without them (Fig. 6). These results indicated that enhancement of humoral immune responses against WT1 was associated with favorable prognosis in patients with NSCLC.

Discussion

In the present study, we showed that WT1 IgG Ab was produced in all of the 91 NSCLC patients and 70 healthy individuals and that 26.4% of the NSCLC patients had WT1 IgG Ab titers over the cut-off level which was mean + 3SD of those of healthy individuals. These findings showed two aspects of WT1 specific immune responses in NSCLC patients. One was that, in consistence with our previous reports on patients with leukemia and MDS,[17,18] humoral immune responses were also elicited against cancer-derived WT1 protein in patients with NSCLC. The elevation of WT1 Ab titers were found even in stage IA NSCLC in which tumor size was less than 3 cm, indicating that the immune system could recognize cancer-derived WT1 protein and respond to it when its amount was still small. Another was the difference in the immune responses against WT1 protein in individual NSCLC patients. No differences were observed in clinical param-

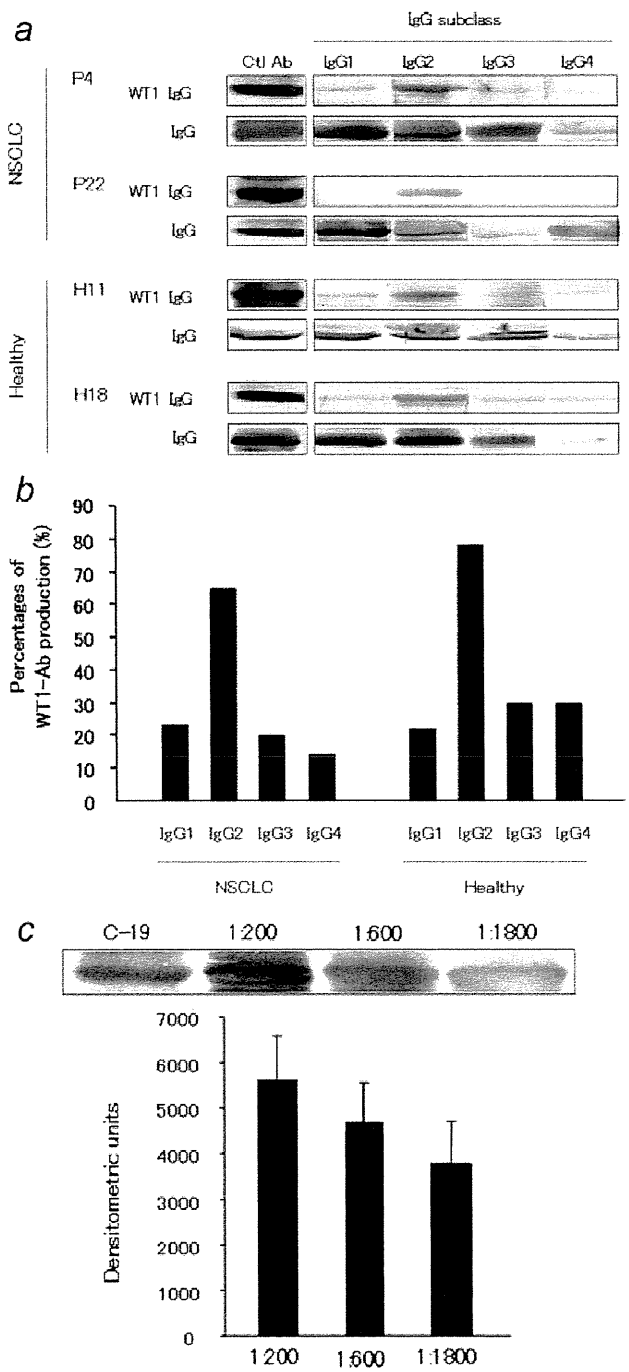

FIGURE 4 – Subclass distribution of WT1 IgG Ab. Recombinant WT1 fragment protein (WT-Fr3, approximately 200 ng/lane) was subjected to Western blot analysis using sera from NSCLC patients and healthy individuals as first antibodies. Membrane bound WT1 IgG Ab was visualized using IgG subclass-specific second Ab. (*a*) Representative results of Western blot analysis for WT1 IgG Ab and IgG subclasses in NSCLC patients (P4 and P22) and healthy individuals (H11 and H18). Results of WT1 IgG Ab (upper panels) and total IgG (lower panels) subclasses were displayed in pairs for each patient and healthy individual. WT1 polyclonal C-19 Ab and IgG Ab were used to confirm the positions of the bands responsible for WT1 IgG Ab and IgG, respectively. (*b*) Positive rate of each subclass of WT1 IgG Ab produced in NSCLC patients and healthy individuals is graphically shown. (*c*) Semiquantitative nature of the Western blot analysis. Western blot analysis was performed for detecting IgG2 WT1 Ab, which was dominantly contained in the serum, by using WT1-Fr3 protein as an antigen and serially diluted serum from a NSCLC patient (P4) (upper). To confirm the band of WT1 IgG Ab, polyclonal WT1 Ab C-19 was used. The band density obtained from the diluted serum is graphically shown as the mean (columns) and SD (bars) of four independent experiments (lower).

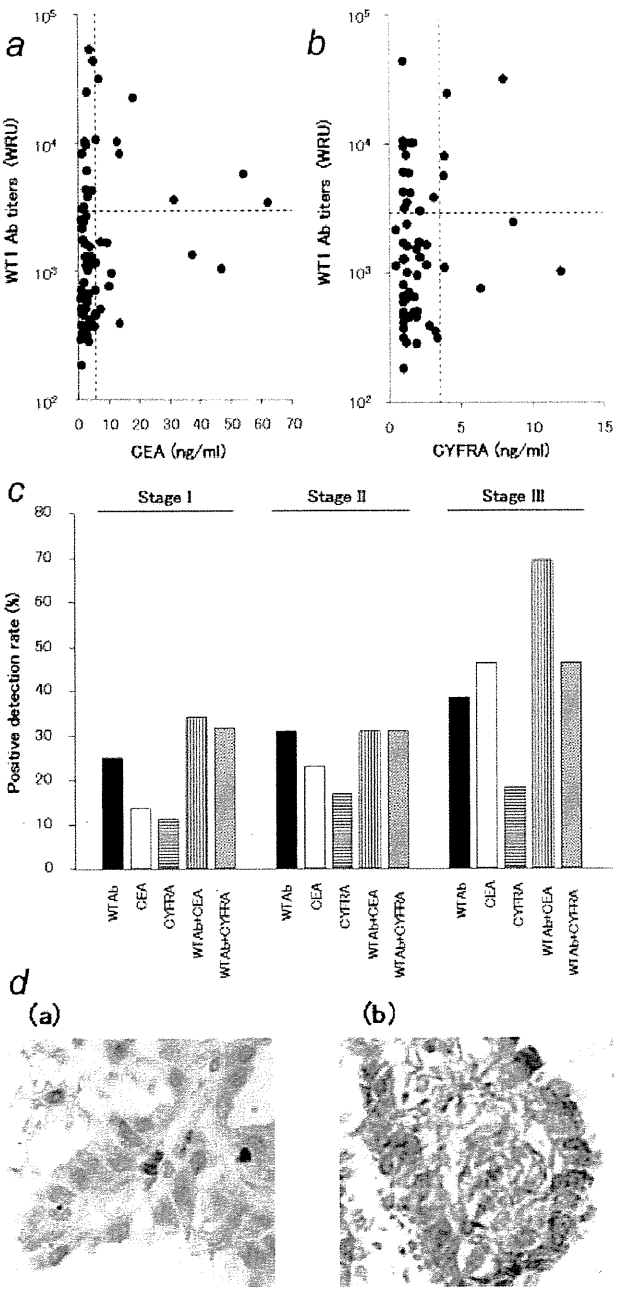

FIGURE 5 – WT1 Ab level as a marker for detection of NSCLC. No correlation between WT1 Ab levels and levels of current NSCLC tumor marker, (*a*) CEA (n = 70) or (*b*) CYFRA (n = 59). Dotted line indicates the cut-off level for each marker. (*c*) Positive detection rate for NSCLC. (*d*) Overexpression of WT1 protein in stage I NSCLC. Expression of WT1 protein was examined by immunohistochemistry in stage I NSCLC. (*a*, *b*) Representative results of different cases are shown. WT1 protein is detected in brown.

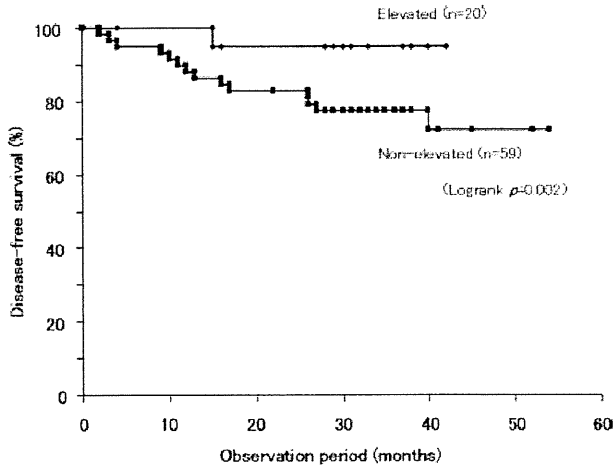

FIGURE 6 – Kaplan–Meier curves for disease-free survival in 79 NSCLC patients. The results from NSCLC patients with elevated WT1 IgG Ab titers (elevated, n = 20) and without them (nonelevated, n = 59) are shown.

eters such as histology, clinical stages and age among NSCLC patients with or without elevated WT1 Ab titers. Thus, the reason why a part of NSCLC patients highly produced WT1 Ab remains undetermined.

There is a great need to develop novel biomarkers for early detection of NSCLC. In the present study, we showed that positive detection rate of WT1 Ab was higher than that of CEA or CYFRA in stages I and II NSCLC. One reason for it should be the difference in the substances measured in these assays. Because the currently available cancer biomarkers such as CEA and CYFRA are based on the measurement of the substances released into blood from cancer cells, detection of such substances may be difficult until cancer becomes advanced and releases considerable amount of the substances. In contrast, measurement of WT1 Ab is an assay of antigen-specific humoral immune responses. Even if early cancer releases small amount of tumor antigens, host immune system is considered to be able to recognize small amount of antigens and respond to them. Through this process, a signal with antigenic tumor protein is biologically amplified to the detectable level.[19] Furthermore, because WT1 Ab was an independent tumor marker that was not correlated with serum levels of CEA and CYFRA, combination of WT1 Ab with CEA or CYFRA increased the positive detection rates for NSCLC. Taken together, these results indicated that WT1 Ab was a useful serum marker for early detection of NSCLC.

Helper T cells are central regulators of both humoral and cellular immune responses.[20] Th1 cells are primarily responsible for activating and regulating the development and persistence of cytotoxic T lymphocyte. In addition, Th1 cells activate antigen-presenting cells and induce the production of Th1 type antibodies (IgG1, 2 and 3), whereas Th2 cells promote that of Th2 type one (IgG4). In the present study, we analyzed the subclass of WT1 IgG Ab and showed that dominant subclass of WT1 IgG Ab was Th1-type IgG2 in NSCLC patients, indicating activation of Th1 type WT1-specific immune responses. These results might indicate that WT1-specific $CD8^+$ cytotoxic T lymphocyte (CTL) responses were more activated in NSCLC patients with elevated WT1 Ab titers compared with those without them. Interestingly, high titers of WT1 IgG Ab were associated with longer DFS in NSCLC patients. This may be explained by the activated WT1-specific $CD8^+$ CTL responses in NSCLC patients with elevated WT1 Ab titers. Another possible explanation is a direct cytotoxic effect of WT1-specific $CD4^+$ T lymphocytes on NSCLC cells. Recently, direct recognition and lysis of leukemia cells by WT1-specific $CD4^+$ T lymphocytes in an HLA class II-restricted manner were reported.[21] Because elevated WT1 Ab titers were considered to be associated with activation of WT1-specific $CD4^+$ T lymphocytes and because HLA class II molecules were expressed in NSCLC cells,[22] it was possible that WT1-specific $CD4^+$ T lymphocytes exert their cytotoxic activities against NSCLC. These findings and our results presented here indicated that WT1-specific immune responses played an important role in anti-tumor immu-

nity against NSCLC and that WT1 IgG Ab was a good marker for prognostic prediction of NSCLC.

Although many reports show the production of antibodies against autoantigens in cancer patients,[23–25] that of these antibodies in healthy individuals remains unclear. This study showed that WT1 IgG Ab was produced in all of the healthy individuals examined. The titers of WT1 IgG Ab in these individuals were low and dominant subclass of WT1 IgG Ab was Th1-type IgG2. Thus, Th1-type humoral immune responses were weakly elicited in healthy individuals. Moreover, our previous report showed that WT1-specific CTLs exist at a percentage of 0.04 ± 0.02% of $CD8^+$ T-cells in peripheral blood mononuclear cells of five healthy volunteers.[26] The frequency seems to be higher than that of CTLs against other antigens such as gp100 or Tyrosinase.[27] These results indicated that WT1 protein elicited both humoral and cellular immune responses in healthy individuals, indicating its high immunogenecity. As for the source of WT1 antigen in healthy individuals, one possible source of WT1 antigen is normal WT1-expressing organs such as urogenital systems and mesothelium.[28] Although these organs express WT1 protein at high levels, no injury was observed in the patients vaccinated with WT1 peptide in clinical trials,[29] suggesting that the normal WT1-expressing organs are protected from WT1-specific immune responses by unknown mechanism. Another source may be undetectable tumors expressing WT1. It is considered that tumors develop in healthy individuals but are eliminated by host immune surveillance system before tumors grow to detectable levels.[30] Because WT1 protein is highly immunogenic, WT1-specific immune responses may function as one of immune surveillance system against cancer in healthy individuals.

Acknowledgements

The authors thank Dr. Yoshinori Iwatani (Department of Biomedical Informatics, Osaka University Graduate School of Medicine) for his advice on ELISA.

References

1. Schrump DS, Altorki NK, Henschke CL, Carter D, Turrisi AT, Gutierrez ME. Cancer: principles and practice of oncology, 7th edn. Philadelphia: Lippincott Williams and Wilkins, 2005;753–810.
2. Bastarrika G, García-Velloso MJ, Lozano MD, Montes U, Torre W, Spiteri N, Campo A, Seijo L, Alcaide AB, Pueyo J, Cano D, Vivas I, et al. Early lung cancer detection using spiral computed tomography and positron emission tomography. Am J Respir Crit Care Med 2005;171:1378–83.
3. Mulshine JL. Clinical issues in the management of early lung cancer. Clin Cancer Res 2005;11:4993s–8s.
4. Burt RW, Ratcliffe JG, Stack BH, Cuthbert J, Kennedy RS, Corker CS, Franchimont P, Spilg WG, Stimson WH. Serum biochemical markers in lung cancer. Br J Cancer 1978;37:714–7.
5. Boddy JJ, Sculier JP, Raymakers N, Paesmans M, Ravez P, Libert P, Richez M, Dabouis G, Lacroix H, Bureau G, Thiriaux J, Lecomte J, et al. Evaluation of squamous cell carcinoma antigen as a new marker for lung cancer. Cancer 1990;65:1552–6.
6. Call KM, Glaser T, Ito CY, Buckler AJ, Pelletier J, Haber DA, Rose EA, Kral A, Yeger H, Lewis WH, Jones C, Housman DE. Isolation and characterization of a zinc finger polypeptide gene at the human chromosome 11 Wilms' tumor locus. Cell 1990;60:509–20.
7. Inoue K, Sugiyama H, Ogawa H, Nakagawa M, Yamagami T, Miwa H, Kita K, Hiraoka A, Masaoka T, Nasu K, Kyo T, Dohy H, et al. WT1 as a new prognostic factor and a new marker for the detection of minimal residual disease in acute leukemia. Blood 1994;84:3071–9.
8. Oji Y, Miyoshi S, Maeda H, Hayashi S, Tamaki H, Nakatsuka S, Yao M, Takahashi E, Nakano Y, Hirabayashi H, Shintani Y, Oka Y, et al. Overexpression of the Wilms' tumor gene WT1 in *de novo* lung cancers. Int J Cancer 2002;100:297–303.
9. Oji Y, Miyoshi S, Takahashi E, Koga S, Nakano Y, Shintani Y, Hirabayashi H, Matsumura A, Iuchi K, Ito K, Kishimoto Y, Tsuboi A, et al. Absence of mutations in the Wilms' tumor gene wt1 in *de novo* non-small cell lung cancers. Neoplasma 2004;51:17–20.
10. Nakatsuka SI, Oji Y, Horiuchi T, Kanda T, Kitagawa M, Takeuchi T, Kawano K, Kuwae Y, Yamauchi A, Okumura M, Kitamura Y, Oka Y, et al. Immunohistrochemical detection of WT1 protein in a variety of cancer cells. Mod Pathol 2006;19:804–14.
11. Oji Y, Yano M, Nakano Y, Abeno S, Nakatsuka S, Ikeba A, Yasuda T, Fujiwara Y, Takiguchi S, Yamamoto H, Fujita S, Kanato K, et al. Overexpression of the Wilms' tumor gene WT1 in esophageal cancer. Anticancer Res 2004;24:3103–8.
12. Oji Y, Yamamoto H, Nomura M, Nakano Y, Ikeba A, Nakatsuka S, Abeno S, Kiyotoh E, Jomgeow T, Sekimoto M, Nezu R, Yoshikawa Y, et al. Overexpression of the Wilms' tumor gene WT1 in colorectal adenocarcinoma. Cancer Sci 2003;94:712–7.
13. Oji Y, Nakamori S, Fujikawa M, Nakatsuka S, Yokota A, Tatsumi N, Abeno S, Ikeba A, Takashima S, Tsujie M, Yamamoto H, Sakon M, et al. Overexpression of the Wilms' tumor gene WT1 in pancreatic ductal adenocarcinoma. Cancer Sci 2004;95:583–7.
14. Sugiyama H. Wilms' tumor gene WT1: its oncogenic function and clinical application. Int J Hematol 2001;73:177–87.
15. Ito K, Oji Y, Tatsumi N, Shimizu S, Kanai Y, Nakazawa T, Asada M, Jomgeow T, Aoyagi S, Nakano Y, Tamaki H, Sakaguchi N, et al. Anti-apoptotic function of 17AA(+)WT1 (Wilms' tumor gene) isoforms on the intrinsic apoptosis pathway. Oncogene 2006;25:4217–29.
16. Jomgeow T, Oji Y, Tsuiji N, Ikeda Y, Ito K, Tsuda A, Nakazawa T, Tatsumi N, Sakaguchi N, Takashima S, Shirakata T, Nishida S, et al. Wilms' tumor gene WT1 17AA(-)/KTS(-) isoform induces morphological changes and promotes cell migration and invasion in vitro. Cancer Sci 2006;97:259–70.
17. Elisseeva OA, Oka Y, Tsuboi A, Ogata K, Wu F, Kim EH, Soma T, Tamaki H, Kawakami M, Oji Y, Hosen N, Kubota T, et al. Humoral immune responses against Wilms' tumor gene WT1 product in patients with hematopoietic malignancies. Blood 2002;99:3272–9.
18. Wu F, Oka Y, Tsuboi A, Elisseeva OA, Ogata K, Nakajima H, Fujiki F, Masuda T, Murakami M, Yoshihara S, Ikegame K, Hosen N, et al. Th1-biased humoral immune responses against Wilms tumor gene WT1 product in the patients with hematopoietic malignancies. Leukemia 2005;19:268–74.
19. Hanash S. Harnessing immunity for cancer marker discovery. Nat Biotechnol 2003;21:37–8.
20. Knutson KL, Disis ML. Tumor antigen-specific T helper cells in cancer immunity and immunotherapy. Cancer Immunol Immnother 2005;54:721–8.
21. Guo Y, Niiya H, Azuma T, Uchida N, Yakushijin Y, Sakai I, Hato T, Takahashi M, Senju S, Nishimura Y, Yasukawa M. Direct recognition and lysis of leukemia cells by WT1-specific $CD4^+$ T lymphocytes in an HLA class II-restricted manner. Blood 2005;106:1415–8.
22. Redondo M, Ruiz-Cabello F, Concha A, Hortas ML, Serrano A, Morell M, Garrido F. Differential expression of MHC class II genes in lung tumour cell lines. Eur J Immunogenet 1998;25:385–91.
23. Cho-Chung YS. Autoantibody biomarkers in the detection of cancer. Biochim Biophys Acta 2006;1762:587–91.
24. Brichory F, Beer D, Le Naour F, Giordano T, Hanash S. Proteomics-based identification of protein gene product 9.5 as a tumor antigen that induces a humoral immune response in lung cancer. Cancer Res 2001;61:7908–12.
25. He P, Naka T, Serada S, Fujimoto M, Tanaka T, Hashimoto S, Shima Y, Yamadori T, Suzuki H, Hirashima T, Matsui K, Shiono H, et al. Proteomics-based identification of alpha-enolase as a tumor antigen in non-small lung cancer. Cancer Sci 2007;98:1234–40.
26. Kawakami M, Oka Y, Tsuboi A, Harada Y, Elisseeva OA, Furukawa Y, Tsukaguchi M, Shirakata T, Nishida S, Nakajima H, Morita S, Sakamoto J, et al. Clinical and immunologic responses to very low-dose vaccination with WT1 peptide (5microgram/body) in a patient with chronic myelomonocytic leukemia. Int J Hematol 2007;85:426–9.
27. Mortarini R, Piris A, Maurichi A, Molla A, Bersani I, Bono A, Bartoli C, Santinami M, Lombardo C, Ravagnani F, Cascinelli N, Parmiani G, et al. Lack of terminally differentiated tumor-specific $CD8^+$ T cells at tumor site in spite of antitumor immunity to self-antigens in human metastatic melanoma. Cancer Res 2003;63:2535–45.
28. Menke AL, van der Eb AJ, Jochemsen AG. The Wilms' tumor 1 gene: oncogene or tumor suppressor gene? Int Rev Cytol 1998;181:151–212.
29. Oka Y, Tsuboi A, Taguchi T, Osaki T, Kyo T, Nakajima H, Elisseeva OA, Oji Y, Kawakami M, Ikegame K, Hosen N, Yoshihara S, et al. Induction of WT1 (Wilms' tumor gene)-specific cytotoxic T lymphocytes by WT1 peptide vaccine and the resultant cancer regression. Proc Natl Acad Sci USA 2004;101:13885–90.
30. Dunn GP, Bruce AT, Ikeda H, Old LJ, Schreiber RD. Cancer immunoediting: from immunosurveillance to tumor escape. Nat Immunol 2002;3:991–8.

Bone Marrow AT_1 Augments Neointima Formation by Promoting Mobilization of Smooth Muscle Progenitors via Platelet-Derived SDF-1α

Hirokazu Yokoi, Hiroyuki Yamada, Yoshinori Tsubakimoto, Hiroki Takata, Hiroyuki Kawahito, Sou Kishida, Taku Kato, Akihiro Matsui, Hideyo Hirai, Eishi Ashihara, Taira Maekawa, Masaru Iwai, Masatsugu Horiuchi, Kouji Ikeda, Tomosaburo Takahashi, Mitsuhiko Okigaki, Hiroaki Matsubara

Objectives—Bone marrow (BM)-derived endothelial progenitor cells (EPCs) and vascular smooth muscle progenitor cells (VPCs) contribute to neointima formation, whereas the angiotensin II (Ang II) type 1 receptor (AT_1)-mediated action on BM-derived progenitors remains undefined.

Methods and Results—A wire-induced vascular injury was performed in the femoral artery of BM-chimeric mice whose BM was repopulated with AT_1-deficient (BM-Agtr1$^{-/-}$) or wild-type (BM-Agtr1$^{+/+}$) cells. Neointima formation was profoundly reduced by 38% in BM-Agtr1$^{-/-}$ mice. Although the number of circulating EPCs (Sca-1$^+$Flk-1$^+$) and extent of reendothelialization did not differ between the 2 groups, the numbers of both circulating VPCs (c-Kit$^-$Sca-1$^+$Lin$^-$) and tissue VPCs (Sca-1$^+$CD31$^-$) incorporated into neointima were markedly decreased in BM-Agtr1$^{-/-}$ mice. The accumulation of aggregated platelets and their content of stromal cell–derived factor-1α (SDF-1α) were significantly reduced in BM-Agtr1$^{-/-}$ mice, accompanied by a decrease in the serum level of SDF-1α. Thrombin-induced platelets aggregation was dose-dependently inhibited (45% at 0.1 IU/mL, $P<0.05$) in Agtr1$^{-/-}$ platelets compared with Agtr1$^{+/+}$ platelets, accompanied by the reduced expression and release of SDF-1α.

Conclusions—The BM-AT_1 receptor promotes neointima formation by regulating the mobilization and homing of BM-derived VPCs in a platelet-derived SDF-1α–dependent manner without affecting EPC-mediated reendothelialization. (***Arterioscler Thromb Vasc Biol.* 2010;30:60-67.**)

Key Words: bone marrow progenitors ■ angiotensin ■ neointima formation ■ stromal cell–derived factor-1α ■ platelet

Bone marrow (BM)-derived progenitors have been shown to contribute to vascular repair and remodeling in both human and animals.[1,2] BM-derived progenitors are mobilized from BM after vascular injury, home into the sites of healing, and differentiate into endothelial-like cells or vascular smooth muscle–like cells, thereby contributing to reendothelialization or neointima formation.[1,2,3,4] Stromal cell-derived factor-1α (SDF-1α) and its receptor CXCR4 were shown to play a crucial role in the mobilization and homing of BM-derived progenitors after injury.[3–7] However, the underlying mechanisms that regulate the serum level of SDF-1α and CXCR4 expression on BM-derived progenitors remain poorly understood.[8]

Angiotensin II (Ang II)-mediated biological actions are involved in the pathogenesis of neointimal hyperplasia after vascular injury.[9,10] Ang II type1 (AT_1) receptor–deficient (Agtr1$^{-/-}$) mice showed attenuated cuff-induced neointima formation.[11] Ang II receptor blocker (ARB) also reduced neointimal hyperplasia in both animal experiments and clinical trials.[12–14] Ohtani et al showed that peripheral blood mononuclear cells (MNCs) isolated from ARB-treated animals showed a decrease in transdifferentiation into smooth muscle-like progenitors.[12] Yamada et al also reported that ARB treatment inhibited neointimal hyperplasia by reducing the accumulation of smooth muscle-like progenitors in neointima.[13] However, the precise mechanisms for AT_1-mediated actions on the mobilization/homing kinetics of BM-derived endothelial progenitor cells (EPCs) and vascular smooth muscle progenitor cells (VPCs) after injury remain poorly defined.

In this study, BM cells of wild-type (WT) were repopulated with Agtr1$^{-/-}$ or Agtr1$^{+/+}$ cells to elucidate the underlying

Received May 27, 2009; revision accepted September 29, 2009.

From the Department of Cardiovascular Medicine, Kyoto Prefectural University School of Medicine, Japan (H. Yokoi, H. Yamada, Y.T., H.T., H.K., S.K., T.K., A.M., K.I., T.T., M.O., H.M.); the Department of Transfusion Medicine and Cell Therapy (H.H., E.A., T.M.), Kyoto University Hospital, Japan; and the Department of Molecular Cardiovascular Biology and Pharmacology (M.I., M.H.), Ehime University Graduate School of Medicine, Japan.

Correspondence to Hiroyuki Yamada, MD, PhD, Department of Cardiovascular Medicine, Kyoto Prefectural University School of Medicine, 465 Kajii-cho, Kamigyo-ku, Kyoto, 602-8566 Japan. E-mail hiyamada@koto.kpu-m.ac.jp

Arterioscler Thromb Vasc Biol **is available at http://atvb.ahajournals.org** **DOI: 10.1161/ATVBAHA.109.192161**

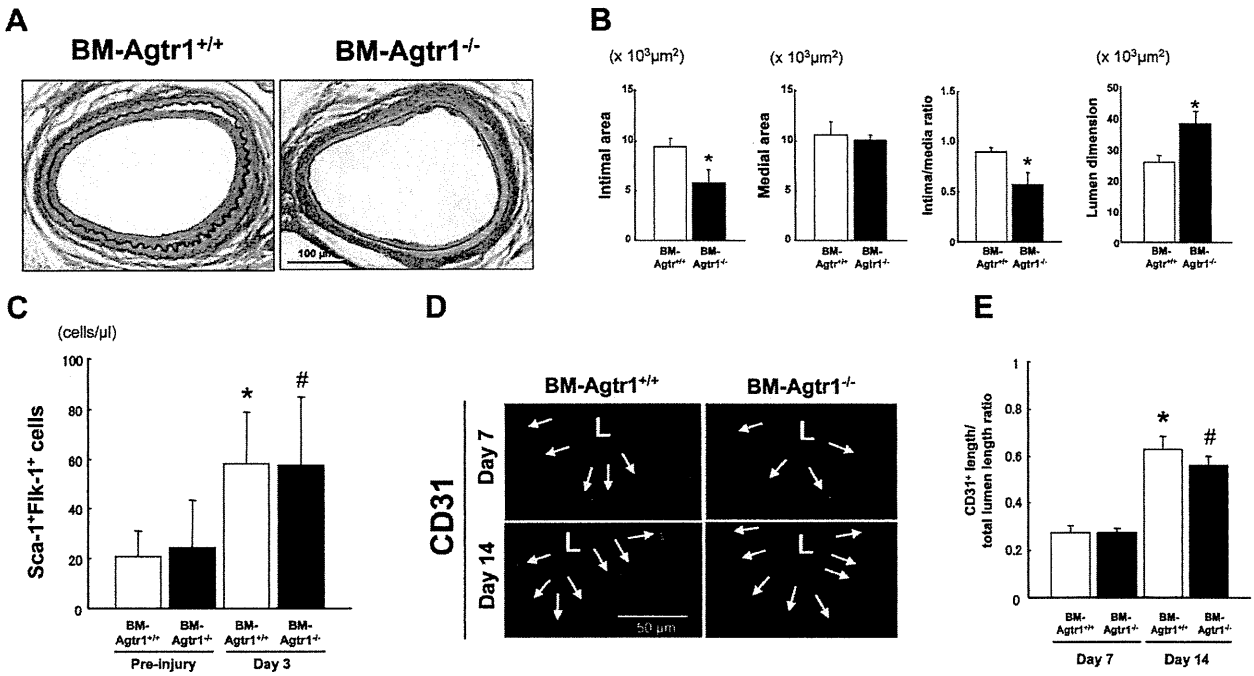

Figure 1. Ablation of marrow AT_1 attenuated neointima formation after vascular injury without affecting on EPC-mediated reendothelialization. A, Representative Elastica van Gieson–stained femoral arteries 4 weeks after injury. B, Quantitative analysis showing significant decreases in neointima formation in BM-Agtr1$^{-/-}$ mice. Values are the mean±SE for at least 8 mice in each group. *P<0.05 vs BM-Agtr1$^{+/+}$ mice. C, Flow cytometry of Sca-1 and Flk-1 expression in circulating mononuclear cell populations 3 days after injury. Quantitative analysis showing no difference in the number of EPCs between the 2 groups before and 3 days after injury. Values are the mean±SE for at least 6 mice in each group. *P<0.05 vs BM-Agtr1$^{+/+}$ mice, #P<0.05 vs BM-Agtr1$^{-/-}$ mice. D, Representative immunohistochemical staining for CD31 at day 7 and day 14 after injury. L indicates lumen. E, Quantitative analysis showing no difference in the extent of reendothelialization between the 2 groups. Values are the mean±SE for at least 6 mice in each group. *P<0.05 vs BM-Agtr1$^{+/+}$ mice, #P<0.05 vs BM-Agtr1$^{-/-}$ mice.

mechanism for BM-AT_1-mediated actions on vascular repair. The results demonstrated for the first time that BM-AT_1 is closely involved in neointima formation by causing the mobilization and homing of VPCs rather than EPCs, in which aggregated platelet-derived SDF-1α plays a crucial role. These findings provide a novel understanding regarding the effect of BM-AT_1 on the kinetics of BM-derived vascular-lineage progenitors after vascular injury especially through platelets AT_1 receptor, and suggest that the BM renin–angiotensin system could be a potential therapeutic target for the vascular remodeling.

Methods

A full description of all methods can be found in the supplemental materials (available online at http://atvb.ahajournals.org).

Animal Preparation

Agtr1$^{-/-}$ mice (C57BL/6 background) were obtained from Tanabe Seiyaku Co Ltd (Osaka, Japan). Vascular injury was performed by inserting a spring-wire into the femoral artery of BM-chimeric mice whose BM was repopulated with AT_1-deficient (BM-Agtr1$^{-/-}$) or wild-type (BM-Agtr1$^{+/+}$) cells. All animal experiments were conducted in accordance with the Guidelines for Animal Experiments at Kyoto Prefectural University School of Medicine.

Results

BM-AT_1 Deficiency Attenuates Neointima Formation After Vascular Injury

The intimal area and intima/media ratio were significantly reduced in BM-Agtr1$^{-/-}$ mice (38% and 33%, respectively, P<0.05), and the lumen dimension was increased (47%, P<0.05) (Figure 1A and 1B). Hemodynamic data and peripheral blood counts data did not differ between the 2 groups (supplemental Tables I and II).

BM-AT_1 Deficiency Does Not Affect Circulating EPCs or Reendothelialization

The number of circulating Sca-1$^+$Flk-1$^+$ EPCs was similarly increased ≈2-fold in both BM-Agtr1$^{+/+}$ and BM-Agtr1$^{-/-}$ mice at day 3 after injury (Figure 1C). The extent of reendothelialization was also equivalent between the 2 groups at day 7 and day 14 after injury (Figure 1D and 1E), suggesting that attenuated neointima formation in BM-Agtr1$^{-/-}$ mice was not attributable to the accelerated re-endothelialization by BM-derived EPCs.

BM-AT_1 Deficiency Inhibits the Mobilization of VPCs

BM-derived VPCs have been shown to contribute to neointima formation after arterial injury,[3,4,12,13] in which

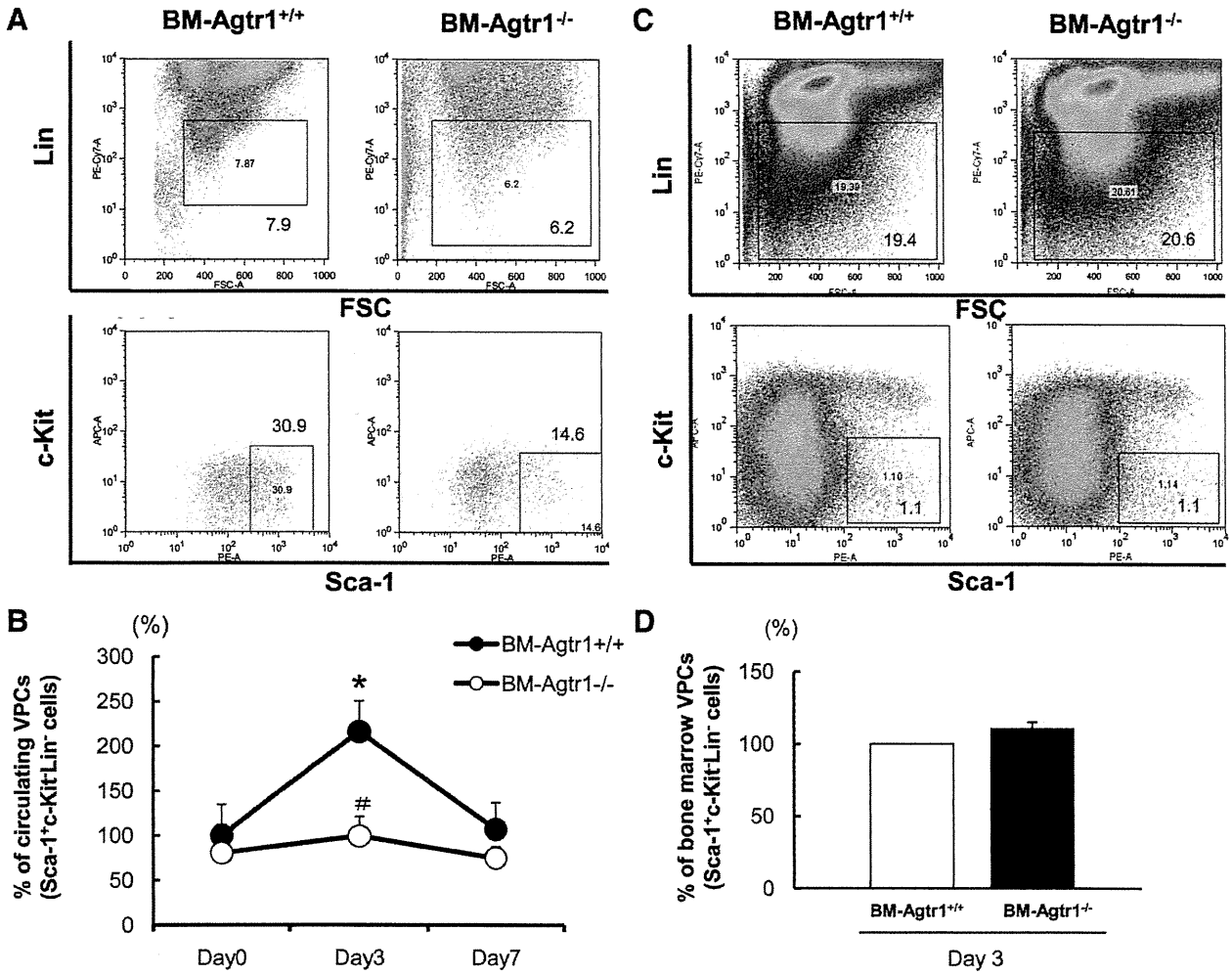

Figure 2. Decreased number of circulating VPCs on ablation of marrow AT_1. A, Flow cytometry of c-Kit and Sca-1 expression in lineage-negative circulating mononuclear cell populations of BM-Agtr1$^{+/+}$ and BM-Agtr1$^{-/-}$ mice before and after injury. B, Quantitative analysis showing the marked increase in the number of circulating VPCs (c-Kit$^-$Sca-1$^+$Lin$^-$) in BM-Agtr1$^{+/+}$ mice at day 3 after injury, whereas a modest increase was observed in BM-Agtr1$^{-/-}$ mice. Values are the mean±SE for 5 mice at each time point in each group. *P<0.05 vs BM-Agtr1$^{+/+}$ mice before injury, #P<0.05 vs BM-Agtr1$^{+/+}$ mice 3 days after injury. C, Flow cytometry of c-Kit and Sca-1 expression in lineage-negative BM populations at day 3 after injury. D, Quantitative analysis showing no difference in the percentage of BM-VPCs of total cells between the 2 groups. Values are the mean±SE for 5 mice in each group.

circulating VPCs were defined as c-Kit$^-$Sca-1$^+$Lin$^-$ cells.[4] We found that the number of circulating VPCs (c-Kit$^-$Sca-1$^+$Lin$^-$) was markedly increased by 117% in BM-Agtr1$^{+/+}$ mice at day 3 after injury (P<0.05), whereas it was completely diminished in BM-Agtr1$^{-/-}$ mice (Figure 2A and 2B). The numbers of BM-VPCs at day 3 after injury were equivalent between BM-Agtr1$^{+/+}$ and BM-Agtr1$^{-/-}$ mice (Figure 2C and 2D), suggesting that the mobilization of VPCs from BM into the circulation was likely to be attenuated in BM-Agtr1$^{-/-}$ mice.

BM-AT_1 Deficiency Reduces Platelet Aggregation and SDF-1α Release

SDF-1α/CXCR4 axis has been shown to play a crucial role in the mobilization of VPCs.[4] The expression levels of CXCR4 on the surface of BM-VPCs did not differ between the 2 chimeric mice (supplemental Figure I). We next examined the vascular expression of SDF-1α and found that SDF-1α–positive staining was remarkably declined in BM-Agtr1$^{-/-}$ mice compared with BM-Agtr1$^{+/+}$ mice 3 days after injury (Figure 3A and 3E). Because aggregated platelets have been shown to secrete SDF-1α on the surface of injured arteries,[15] the extent of aggregated platelets and their colocalization with SDF-1α were examined. One day after injury, the inner surface of the injured artery was uniformly covered by platelets, as indicated by CD41 (platelet integrin αIIb)-positive staining, which was almost equivalent between the BM-Agtr1$^{-/-}$ and BM-Agtr1$^{+/+}$ mice (Figure 3B and 3F), suggesting that primary platelet adhesion was not affected by platelet AT_1 deficiency. In contrast, fibrinogen-positive staining, which reflects the fibrinogen trapped by aggregated platelets, was broadly detected in BM-Agtr1$^{+/+}$ mice 3 days after injury, whereas it was apparently diminished in BM-Agtr1$^{-/-}$ mice (Figure 3C and 3G). The expression level of GPIIb mRNA was remarkably reduced by 36% in BM-Agtr1$^{-/-}$ mice compared with BM-Agtr1$^{+/+}$ mice (Figure 3H),

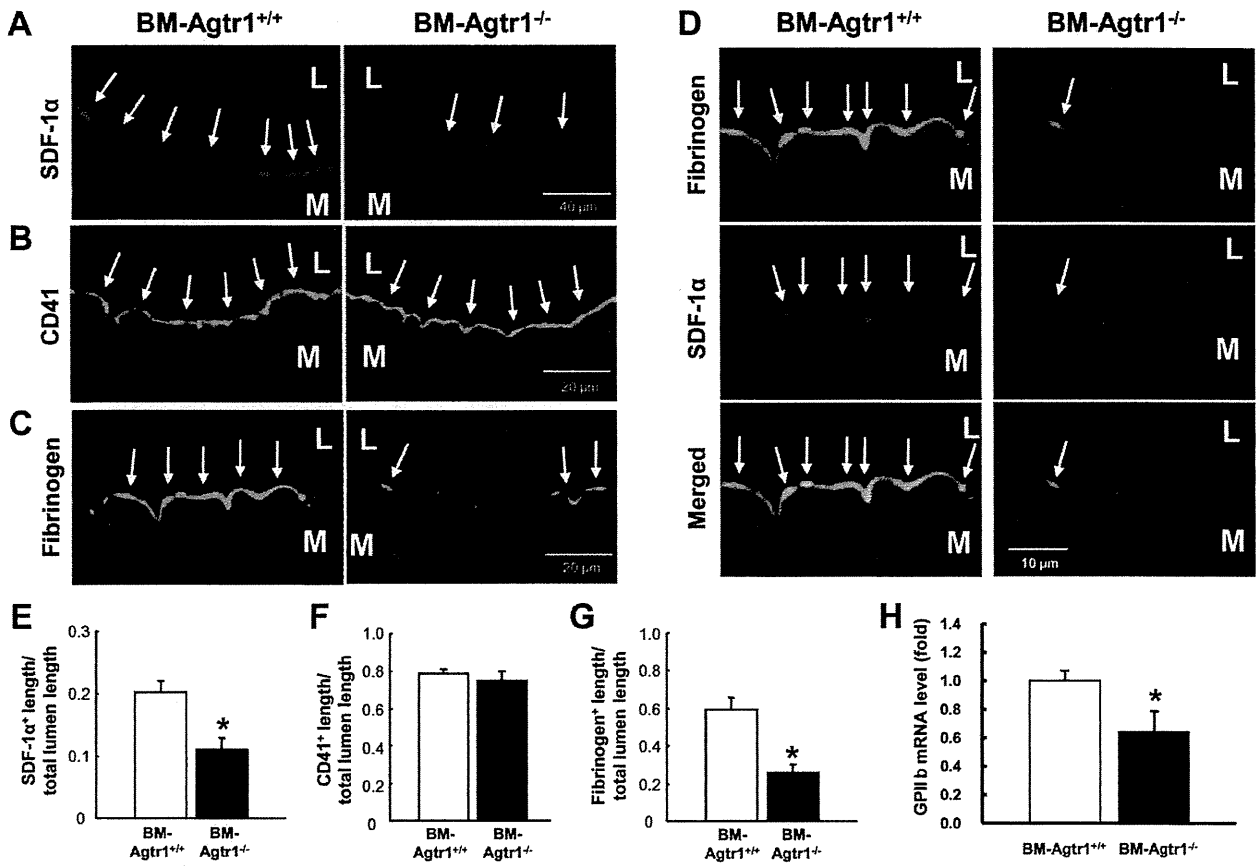

Figure 3. Attenuated platelet aggregation and the content of SDF-1α on ablation of marrow AT_1. A, Immunofluorescence image showing SDF-1α 3 day after injury. SDF-1α–positive staining was mainly detected on the inner surface of the vessel wall. B and C, Immunofluorescence image showing CD41 and fibrinogen at day 1 and day 3 after injury, respectively. D, Merged image showing fibrinogen (green) and SDF-1α (red). E, F, and G, Quantitative analysis showing a decrease in SDF-1α and fibrinogen-positive staining but not in CD41-positive staining in BM-Agtr1$^{-/-}$ mice. Values are the mean±SE for at least 5 mice in each group. *P<0.01 vs BM-Agtr1$^{+/+}$ mice. L indicates lumen; M, media. H, Real-time PCR analysis showing the reduced expression of GPIIb in BM-Agtr1$^{-/-}$ mice. Total RNA was isolated from the injured arteries at day 3, and GPIIb mRNA levels were shown as values relative to BM-Agtr1$^{+/+}$ mice. Values are the mean±SE for at least 5 mice in each group. *P<0.05 vs control BM-Agtr1$^{+/+}$ mice.

supporting the notion that platelets aggregation in the injured vessels is attenuated in BM-Agtr1$^{-/-}$ mice. Moreover, SDF-1α–positive staining was mostly colocalized with fibrinogen-positive staining (Figure 3D), suggesting that diminished platelets aggregation contributes to the decreased content of SDF-1α at sites of injured vessel in BM-Agtr1$^{-/-}$ mice. We also examined the relationship between eNOS and SDF-1α, because SDF-1α has been reported to have a deep relationship to NO synthase.[8] Immunohistochemical analysis showed that CD31-positive endothelium was hardly observed in the inner layer of the injured vessels 3 days after injury, in which colocalization of aggregated platelets and SDF-1α was observed (supplemental Figure IIA). Consistent with this finding, the expression level of eNOS mRNA was much lower in the wire-injured vessels compared with the uninjured contralateral vessels, and the expression levels of eNOS mRNA in the wire-injured vessels did not differ between BM-Agtr1$^{+/+}$ and BM-Agtr1$^{-/-}$ mice (supplemental Figure IIB). These findings suggest that eNOS is unlikely involved in the production of aggregated platelet-derived SDF-1α in our wire-mediated endothelium injury model, compared with the artery ligation model in which endothelium is preserved.[8]

BM-AT_1 Deficiency Decreases the Serum Level of SDF-1α

To further elucidate the causal relationship between aggregated platelet-derived SDF-1α and the mobilization of VPCs, we examined the localization of SDF-1α in the injured vessels and the time course of serum levels of SDF-1α. The serum SDF-1α levels in both BM-Agtr1$^{+/+}$ and BM-Agtr1$^{-/-}$ mice were significantly increased as rapid as 6 hours after injury and thereafter decreased (Figure 4A). Consistent with the findings demonstrated by Zernecke et al, our immunohistochemical analysis at 6 hours after injury showed that SDF-1α–positive staining was observed in the medial wall (data not shown), suggesting that medial smooth muscle cells were the major source of SDF-1α at the acute phase after injury. Thereafter, the serum SDF-1α level in BM-Agtr1$^{+/+}$ mice gradually declined but was still higher than the baseline level 24 hours after injury and thereafter reverted to the baseline at 3 days. In contrast, the serum SDF-1α level in